Honors ThesesHonors College

5-2020

Co-assembly behavior of neutral and zwitterionic amphiphilic block copolymers in the fabrication of glassy polymer vesicles

Elina Ghimire

The University of Southern Mississippi

Co-assembly behavior of neutral and zwitterionic amphiphilic block copolymers in the
fabrication of glassy polymer vesicles

by

Elina Ghimire

A Thesis
Submitted to the Honors College of The
University of Southern Mississippi in
Partial Fulfillment
of Honors Requirements

May 2020

Approved by:

_____
Yoan C. Simon, Ph.D., Thesis Adviser
Professor of Polymer Science

_____
Derek L. Patton, Ph.D., Director
School of Polymer Science and Engineering

_____
Ellen Weinauer, Ph.D., Dean
Honors College

Abstract

Polymersomes, also known as polymer vesicles, are hollow capsules fabricated through the solution assembly of amphiphilic block copolymers. Polymer vesicles have garnered a great deal of interest in materials science because of their potential application in areas such as drug delivery, diagnostics and imaging, gene therapy, and as nanoreactors. The goal of this project is to understand the factors that affect the arrangement of triblocks in vesicle membrane via the study of the co-assembly behavior of linear amphiphilic triblocks with different hydrophilic blocks. We investigated the self- and co-assembly behavior of amphiphilic triblock copolymers with neutral hydrophilic blocks. Moreover, we compared the results obtained from the assembly of neutral triblocks to the self-assembly of zwitterionic and anionic triblock copolymers. First, a central hydrophobic poly(styrene-*stat*-coumarin methacrylate) (P(S-*stat*-CMA) block was synthesized by reversible addition-fragmentation chain-transfer (RAFT) copolymerization of the corresponding monomers using a difunctional chain transfer agent. The two neutral hydrophilic blocks *N,N*-dimethylacrylamide and poly(ethylene glycol) were added by the chain-extension and thio-Michael addition respectively. The zwitterionic [2-(methacryloyloxy)ethyl]dimethyl-(3-sulfopropyl)ammonium hydroxide and the anionic sodium 4-styrene-sulfonate were also obtained via chain extension RAFT polymerization. The variations in sizes, orientation, and distribution patterns of the morphological structures characterized via light scattering and transmission electron microscopy are discussed.

Keywords: Polymer vesicles, RAFT polymerization, self-assembly

Dedication

To my family.

Acknowledgements

I express my sincerest gratitude to my thesis advisor, Dr. Yoan C. Simon, for helping me build a foundation in research. I would also like to pay my special regards to my graduate mentor, Tamuka Chidanguro, for all the help and support during my research journey. Moreover, I would like to acknowledge Drapeau Center for Undergraduate Research for partial financial support of this research. I would like to thank Ying Xiao at Louisiana State University for her help with TEM imaging.

Table of Contents

List of Tables

List of Schemes

List of Figures

List of Abbreviations

AIBN	2,2′-azobis(2- methylpropionitrile)
ATRP	Atom-transfer radical polymerization
CEP	4-cyano-4-(ethylsulfanylthiocarbonyl)sulfanylpentanoic acid
CMA	7-(2-methacryloyloxyethoxy)-4-methylcoumarin
diCEP	Di-4-cyano-4-(ethylsulfanylthiocarbonyl)sulfanylpentanoicacid
DCC	*N,N′*-Dicyclohexylcarbodiimide
DCM	Dichloromethane
DLS	Dynamic Light Scattering
DMAP	4-Dimethylaminopyridine
DMAPS	[2-(methacryloyloxy)ethyl]dimethyl-(3-sulfopropyl)ammonium hydroxide
DMF	*N,N′*-Dimethylfomamide
HFIP	Hexafluoroisopropanol
HHH	Hexagonally packed hollow hoops
LCM	Large compound micelles
NaI	Sodium iodide
NMP	Nitroxide-mediated polymerization
NMR	Nuclear Magnetic Resonance
NaSS	Sodium-4-styrenesulfonate
PEG	Poly (ethylene glycol) acrylate
PS-*stat*-PCMA	Poly(styrene-*stat*-coumarin methacrylate)
RAFT	Reversible addition-fragmentation chain-transfer polymerization
SEC	Size Exclusion Chromatography
SLS	Static Light Scattering
TEM	Transmission Electron Microscopy
THF	Tetrahydrofuran
V-501	4,4'-azobis(4-cyanopentanoic acid)

Chapter 1

Introduction and Statement of Problem

Over the past two decades, polymer vesicles (polymersomes) have attracted a great deal of

interest in materials research, given their potential in various applications. Polymer vesicles are

hollow capsules obtained by the assembly of amphiphilic block copolymers. Typically, polymer

vesicles possess a hydrophobic wall and a hydrophilic corona and lumen. Beyond drug delivery,

they have proven to be useful in fields like biosensing,[30] imaging and diagnostics,[31] and as

nanoreactors.[31] More recently, the potential applications of polymer vesicles have been extended

in areas such as water remediation,[2,3] construction materials,[4] and catalysis.[5] The attraction

towards polymer vesicles is because of their intrinsic hollow nanostructure and the ability to

tailor their architecture and membrane functionalities.[6] Consequently, polymer vesicles can

function as dual-purpose systems by allowing the simultaneous encapsulation of hydrophilic

cargo in their aqueous cavities and incorporation of hydrophobic molecules on the membrane.[6]

Polymer vesicles are the analogues of liposomes, which are composed of one or more

phospholipid bilayers and are widely studied for drug delivery applications. However, despite

their biocompatibility and biodegradability, liposomes do not exhibit good stability and solidity

since they are made up of low molecular weight phospholipids.[7] On the other hand,

polymersomes can be obtained from high molecular weight polymers which impart toughness

and better stability to the structures. Also, the membranes of the polymersomes are generally less

permeable and less fluidic making them physically and chemically stable, which is indispensable

for drug encapsulation purposes.[8]

Most commonly, polymer vesicles are obtained by the assembly of amphiphilic diblock or

triblock copolymers. However, other species such as amphiphilic dendrimers, polypeptides,

1

glycopeptides, and charge balancing surfactants have also been used to fabricate polymer vesicles.[1,21] Beside polymer vesicles, a variety of other morphologies such as micelles, large compound micelles, small and large lamellae, and rods can be formed from the assembly of block copolymer systems under various conditions.[6] Polymer vesicles have particularly been the topic of interest because of the possibility to extensively tailor their membrane properties, thus enabling the pathways for diverse applications. Palivan et. al reviewed the conditions for vesicle fabrication in which they typically mention the use of soft hydrophobic blocks such (poly (dimethyl siloxane), poly (ethylethylene), and poly (butadiene) targeting biomedical applications.[37] Polymer vesicles with glassy membrane were less desired because of their lack of fluidity.[22] However, recently it has been discovered that glassy polymer vesicles have potential in biomedical applications because of their impermeable membrane and their ability to form metastable morphologies.[22] In this project, polymer vesicles with a glassy membrane (polystyrene) are studied.

Although polymersomes have been extensively studied for their ion transport properties and stimuli-responsive applications, there are very few systems capable of controlling the passage across their membrane to prompt anticipated reactions. Particularly, little work has been done to transduce mechanical forces to control the state of ion channels in polymersomes. In order to devise an intricate vesicular system capable of this feat, it is important to observe the co-assembly behavior of linear amphiphilic triblocks in the fabrication of polymer vesicles to control their responsiveness. The overall goal of this project was to study the co-assembly behavior of linear amphiphilic triblock copolymers in the fabrication of polymer vesicles. To do this, two neutral triblocks, with the same composition of the central hydrophobic block but differing in their hydrophilic composition were self- and co-assembled. Later, the project was

extended to understand the influence of electrostatic interaction during the assembly of the block copolymers. Accordingly, an anionic triblock and a zwitterionic triblock, with the same composition of central hydrophobic block as that of neutral triblocks, were synthesized and self-assembled.

1.1. Block copolymers: Introduction and Synthesis

Block copolymers are a specific category of copolymers, in which blocks of chemically different monomer units are aligned linearly along the polymer chain.[9] The blocks are covalently bound and are usually immiscible.[10] Block copolymers can be further subcategorized depending upon the number of distinct blocks and their arrangements. If A and B are considered as the two different monomer units, then they can be arranged in numerous fashions to obtain various architectural structures of block copolymers such as linear diblock (AB), triblock (ABA), pentablock (ABABA), multiblock or segmented copolymers $(AB)_n$ and star diblocks $(AB)_nX$.[11] Additionally, a third type of monomer unit C can be incorporated to obtain triblock structures (ABC).[10] Similarly, other monomer units can be added to obtain multiblock copolymer systems. In general, block copolymers are synthesized either by covalently coupling the different polymeric chains at the respective ends or by the sequential addition of monomers via "living"/controlled polymerization techniques.[12]

Controlled polymerization is a highly favored method of block copolymer synthesis because of its various advantageous features such as wide range of monomer compatibility, high tolerance of functional groups and impurities, and a simpler experimental setup.[9] This method works on the basis that reversible reaction between the active species and the dormant species is used to maintain the reactive polymer chain end.[9] Polymerization methods such as atom transfer

radical polymerization (ATRP),[32] nitroxide-mediated polymerization (NMP),[33] and reversible

addition-fragmentation chain-transfer (RAFT) radical polymerization[23] have been frequently

used for the preparation of block copolymers.[9]

1.2. RAFT polymerization

RAFT polymerization is a versatile reversible deactivation radical polymerization

technique. It can be used to polymerize a wide range of monomers in different reaction

conditions to obtain polymers with controlled molecular weight and narrow polydispersity.[13]

RAFT is different from other reversible deactivation radical polymerization techniques such as

ATRP and NMP because it relies on a degenerative chain-transfer process and does not make use

of persistent radical effect to establish control.[13] As shown in Scheme 1, in RAFT

polymerization, a reversible addition-fragmentation occurs in which the transfer of the S=C(Z)S-

moiety between active and dormant chains serve to maintain the living character of the

polymerization.[13] A suitable chain-transfer agent, typically a thiocarbonylthio group, is

employed in RAFT polymerization. With a proper selection of reagents (chain transfer agent,

initiator, and monomer), nonionic, cationic, anionic, and zwitterionic species can be polymerized

by RAFT under aqueous conditions to obtain their homopolymers as well as block copolymers.[13]

The mechanism of RAFT polymerization involves multiple steps such as initiation, propagation,

RAFT pre-equilibrium, re-initiation, RAFT main equilibrium, and termination. During initiation,

the initiator is decomposed to form radical species. The radical then reacts with the monomer to

form a propagating chain. The active propagating chain with n monomer units (P_n) reacts with

the RAFT agent to enter equilibrium between active and dormant species. Then, degenerative

chain transfer occurs in which reversible transfer of the functional chain end-group takes place

between the propagating radicals and the dormant chains.[23] In general, the rate of

addition/fragmentation occurs at a higher rate than that of propagation, which results in a lower

dispersity.[23] Termination occurs either by coupling or disproportionation.
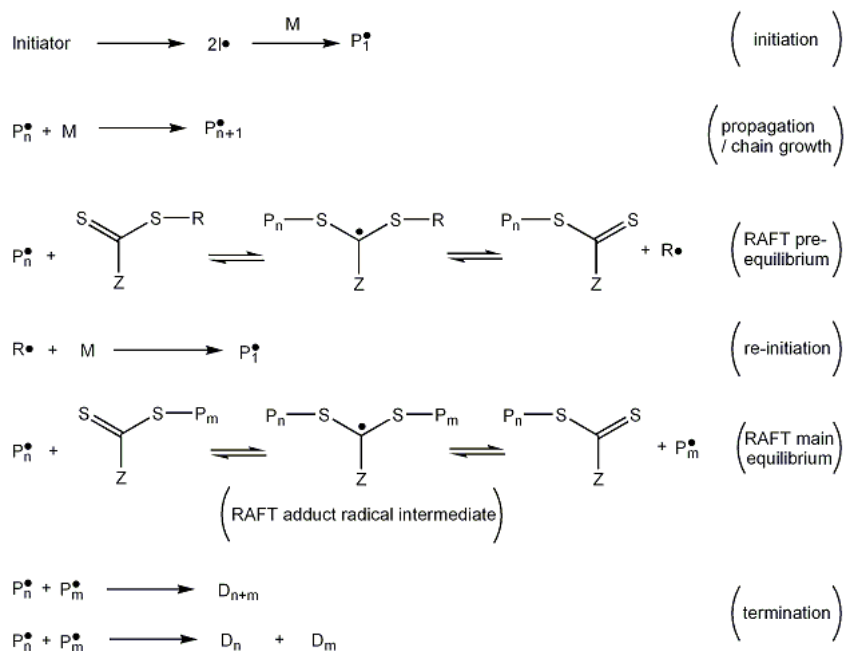
Scheme 1. General scheme of RAFT polymerization

1.3. Self-assembly of block copolymers

1.3.1. Self-assembly in bulk

In bulk, block copolymers with immiscible blocks self-assemble due to microphase

separation as a result of unfavorable mixing enthalpy coupled with a small mixing entropy.[24]

Depending on various factors such as Flory-Huggins interaction parameter (χ), the volume

fraction (Φ), and the total degree of polymerization (N), a variety of morphologies can be

obtained.[9] Spheres, cylinders, gyroids, and lamellae are some of the morphologies obtained as a

result of block copolymer self-assembly in bulk.[9] Self-assembly of block copolymers in bulk has

been studied for potential applications in semiconductors to increase band gap, for fuel-cell applications, nanomaterial templating, and nanoparticle synthesis.[24]

1.3.2. Self-assembly in solution

Comparatively, self-assembly of block copolymers in solution is much more complicated than the self-assembly of block copolymers in bulk because of the addition of solvents which increases the number of χ parameters.[6] Water is the most commonly used solvent in block copolymer self-assembly; depending upon the solubility of the blocks in water, block copolymers can be categorized as amphiphilic,[6,35] double hydrophobic,[36] and double hydrophilic.[35] Amphiphilic block copolymers, with covalently bound hydrophobic and hydrophilic blocks, are extensively studied for self-assembly applications.[34] The self-assembly of amphiphilic block copolymers in solution can result in a plethora of morphologies such as spherical micelles, cylindrical or wormlike micelles, bicontinuous rods, hexagonally packed hollow (HHH) loop, vesicles, lamellae, and large compound micelles (LCM).[6] Figure 2 shows the TEM images of the morphologies obtained from the assembly of amphiphilic polystyrene-block-poly(acrylic acid) (PS_m-b-PAA_n). The formation of different morphologies is determined by the packing parameter $p = \left(\frac{v}{a_0 l_c}\right)$ of the system , where v is the volume of the hydrophobic block, a_0 is the contact area of the head group, and l_c is the length of the hydrophobic block.[9] The packing parameter of the system is influenced by factors such as concentration and composition of block copolymer, solvent mixtures, additives, and ratio of aqueous to organic solvent.[9]

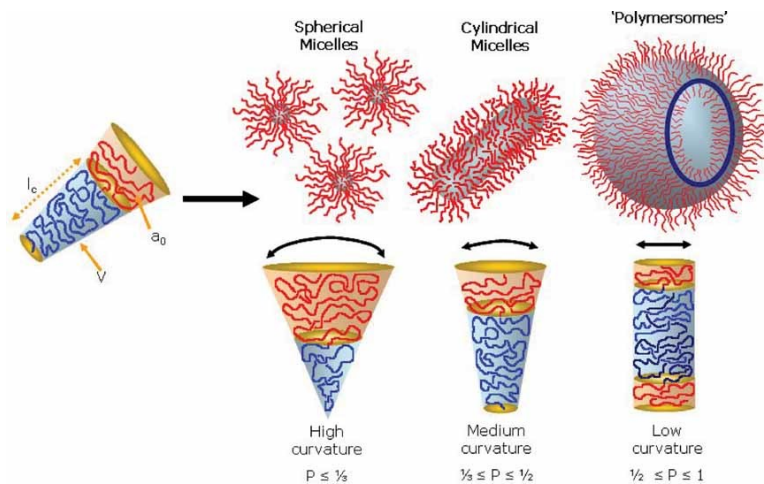**Figure 1.** Various morphologies obtained by the self-assembly of amphiphilic block copolymer. The morphologies are formed based on the inherent curvature of the molecules, which is determined by the calculation of packing parameter, p [25]
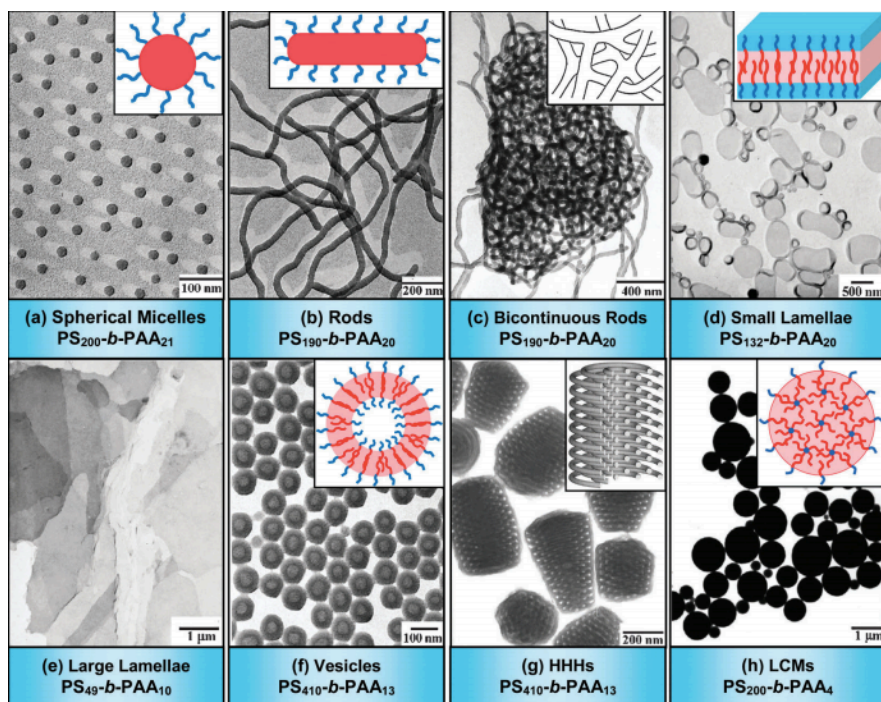

Figure 2. TEM images of the morphologies obtained from the assembly of amphiphilic (PS_m-b-PAA_n), where m and n are the degrees of polymerization of PS and PAA. [6]

1.4. Zwitterionic polymers in block copolymer self-assembly

Zwitterionic polymers are interesting synthetic analogues for proteins, given the fact that they possess both positive and negative charges.[14] In zwitterion-bearing amphiphilic block copolymers, two oppositely charged electrolyte chains can form a robust electrostatic complex due to the increased entropy of the released small anions and cations.[14] In addition, zwitterionic polymers behave as polar non-ionic polymers, despite the fact that they are charged.[14] Polyzwitterions can be designed into stimuli-responsive polymeric systems because they show an upper critical solution temperature in aqueous media.[14] Such systems can be reversibly sensitive to changes in temperature, ionic strength, specific ion pairing, and chemical reactions.[14,26]

Compared to the conventional nonionic polymeric systems, fewer works have been done with zwitterion-bearing systems, particularly in the field of assembled morphologies. The majority of reports have hydrophilic blocks composed of nonionic poly(ethylene oxide) or charged poly(acrylic acid), while polymers such as polystyrene, poly(lactic acid), polycaprolactone and polybutadiene compose the hydrophobic block.[15] Zwitterions resemble natural functional groups such as phosphatidylcholines, and therefore are thought to be biocompatible.[14] Zwitterionic polymers, consisting of an equal number of positive and negative charges, possess some outstanding properties that make them applicable in areas such as anti-fouling coatings, hydrogel materials, dispersants and stabilizers, antifreeze materials, and in drug delivery and gene therapy.[17] Despite their many interesting characteristics, only a few studies have focused on zwitterion-bearing polymers in the formation of polymer vesicles.[15,27] Moreover, the fabrication of polymer vesicles from zwitterionic polymers is mainly based on diblock systems.[15,27,28] And there are very few works that are based on zwitterionic triblock

systems.[29] Therefore, the study and comparison of the polymer vesicles obtained from the neutral and ionic triblock copolymer systems will help to understand the influence of electrostatic and hydrophobic interaction in the assembly behavior.

1.5. Research Overview

The primary goal of this project was to understand the distribution pattern of amphiphilic triblock copolymers throughout the membrane of the vesicles. The insights gained from the project will help to precisely control the position of synthetic gates on the membrane of the vesicles. Herein, we synthesized two neutral triblocks and self- and co-assembled them into polymer vesicles. Both of the triblocks contained the same composition of hydrophobic block in the center, which was obtained by the RAFT polymerization of styrene and coumarin methacrylate (CMA). CMA was chosen as one of the monomers because of its ability to dimerize which would permanently lock the membrane integrity. After the study of the assembly behavior of neutral triblocks, the project was extended to the study of ionic polymers, to understand the influence of electrostatic interaction during the assembly of amphiphilic block copolymers.

Chapter 2

Experimental Methods

2.1. Materials

The monomer precursors 7-(2-hydroxyethoxy)-4-methylcoumarin (Alfa Aesar, 97%), ethylene carbonate (Acros, 99+%), triethylamine (Fisher Chemical, reagent grade), and sodium sulfate (Fisher Chemical) were used as received. Methacryloyl chloride (Aldrich, 97%) was stored at -10 ^{o}C prior to use. The RAFT agent precursors sodium hydride (Acros), ethane thiol (Acros, 97+%), carbon disulfide (Sigma Aldrich), I$_2$ (Acros), sodium thiosulfate (Fisher Scientific), 4,4′-azobis(4- cyanopentanoic acid) (V-501) (Alfa Aesar), ethylene glycol (Fisher Sceintific), *N,N'*-dicyclohexylcarbodiimide (DCC) (Avocado Research Chemicals), and 4-dimethylaminopyridine (DMAP) (Acros) were used as received. The monomers *N,N*-dimethylacrylamide (Sigma Aldrich), sodium 4-styrenesulfonate (NaSS) (Aldrich), 2000g/mol poly(ethylene glycol) acrylate (Sigma Aldrich) and [2-(methacryloyloxy)ethyl]dimethyl-(3-sulfopropyl)ammonium hydroxide (DMAPS) (Aldrich, 95%) were used as received. Hexylamine (Acros, 99%), and tributylphosphine (Sigma Aldrich) were used as received. The solvents hexafluoroisopropanol (Chem-impex, 99.9%), dimethylfomamide (DMF) (Fisher Chemical), chloroform (Fisher Chemical), dichloromethane (Fisher Chemical), diethyl ether (Fisher Scientific), and pentane (Fisher Scientific) were used as received. The initiator 2,2′-azobis(2-methylpropionitrile) (AIBN) (Sigma Aldrich, 96%) was recrystallized in methonal prior to use. The detailed synthesis of RAFT agent (diCEP) and monomer (CMA) are described below.

2.2. Synthesis of 7-(2-methacryloyloxyethoxy)-4-methylcoumarin (CMA)

Using a procedure as previously reported,[18] 7-(2- hydroxyethoxy)-4-methylcoumarin was synthesized. In 40 mL of DMF, 7-hydroxy-4-methylcoumarin (8.8 g, 50 mmol, 1.0 equiv.) and ethylene carbonate (4.4 g, 50 mmol, 1.0 equiv) were dissolved. Then, potassium carbonate (13.8 g, 100 mmol, 2.0 equiv) was added and the mixture was stirred under nitrogen at 100 °C for overnight. The product was precipitated in 500 mL mixture of ice and deionized water and collected via vacuum filtration. After drying in a vacuum oven, yellowish powder was obtained with a yield of 85%. ^{1}H NMR (300 MHz, DMSO-d_6, δ, ppm): 7.70–7.60 (m, 1H), 7.00–6.89 (m, 2H), 6.18 (d, 1H), 4.91 (t, 1H), 4.08 (t, 2H,), 3.73 (dd, 2H), 2.38 (d, 3H).

CMA was synthesized according to the literature.[19] 7-(2- Hydroxyethoxy)-4-methylcoumarin (8.00 g, 36.3 mmol, 1.0 equiv) was dissolved in 100 mL chloroform. Triethylamine (10.13 mL, 72.65 mmol, 2.0 equiv) was added and the mixture was stirred at 0 °C for 15 minutes. Then, methacryloyl chloride (7.097 mL, 72.65 mmol, 2.0 equiv) was added to the mixture dropwise at 0 °C under nitrogen atmosphere for 16 hours. Dichloromethane was added to the reaction mixture and the organic layer was washed with 50 mL of brine twice. The organic layer was then dried over sodium sulfate and the solvent was removed via rotary evaporation. The crude product was recrystallized from ethanol to obtain white powdery crystals with a yield of 65%. ^{1}H NMR (300 MHz, CDCl₃, δ, ppm): 1.96 (s, 3H), 2.4 (s, 3H), 4.28 (t, 2H), 4.53 (t, 2H), 5.60 (s, 1H), 6.15 (s, 1H), 6.8–6.9 (m, 2H), 7.5 (d, 1H).

2.3. Synthesis of di-4-cyano-4-(ethylsulfanylthiocarbonyl)sulfanylpentanoic acid (diCEP)

A suspension of (95%) NaH (2.11 g, 83.5 mmol) in anhydrous diethyl ether (150 mL, 1.42 mol) and was cooled to 0 °C using an ice bath. Then, ethane thiol (5.73 g, 92.3 mmol) was

slowly added over 15 min followed by vigorous evolution of hydrogen gas. The reaction was stirred for an additional 15 min at 0 °C, followed by dropwise addition of carbon disulfide (7.03g, 92.3 mmol) over 5 min. The reaction was stirred for 60 min at room temperature. The heterogenous mixture was then diluted with pentane (100 mL), which resulted in a yellow precipitate. The precipitate was isolated by vacuum filtration before drying in-vacuo, yielding sodium ethyl trithiocarbonate. Sodium ethyl trithiocarbonate (9.89g, 61.7 mmol) was suspended in diethyl ether (200 mL) at room temperature, which was followed by the addition of solid I_2 (8.63g, 34.0 mmol) over 5 min. The reaction was stirred for 60 min at room temperature and sodium iodide (NaI) salts were precipitated. The precipitated NaI salts were removed by vacuum filtration and washed with 50 mL diethyl ether. The filtrate was transferred to a separatory funnel and washed with 5% sodium thiosulfate (2 x 150 mL), H_2O (1 x 150 mL), and brine (1 x 150 mL) before drying over magnesium sulfate. The solvent was removed via rotary evaporation followed by drying in-vacuo to yield bis(ethyl) trithiocarbonate as a yellow solid. A solution of bis-ethyltrithiocarbonate (5.00g, 18.2 mmol) and 4,4′-Azobis(4-cyanopentanoic acid) (V-501) (7.66g, 27.3 mmol) in EtOAc (250 mL) was prepared in a 500 mL 3-necked flask equipped with stir bar and condenser. The solution was purged with N2 for 45 mins which was then heated t reflux for 18 hours. The reaction was quenched via exposure to air and cooled to room temperature. The solvent was removed via rotary evaporation and the crude RAFT agent purified via column chromatography on SiO2 (60:35:5 Hexanes:EtOAc:Acetic acid). To remove the acetic acid, the column fractions containing CEP were combined and transferred to a separatory funnel and washed with 0.05N HCl (2 x 150 mL), brine (1 x 150 mL), dried over MgSO4, and the solvent removed via rotary evaporation followed by drying in-vacuo to yield CEP as a yellow solid.

Yield: 7.10 g (74%); 1H NMR (300 MHz, CDCl3, δ, ppm): 3.38 (q, 2H), 2.70 (t, 2H), 2.55 (m, 2H), 1.85 (s, 3H), 1.40 (t, 3H)

In a 100 mL two-necked flask, CEP (2.09g, 7.96 mmol) was added under nitrogen atmosphere. Then, ethylene glycol (0.22g, 3.62 mmol) was added to the flask followed by the addition of 30 mL of dichloromethane (DCM). The mixture was stirred in an ice and water bath under nitrogen. Dicyclohexyldiimide (DCC) (1.56g, 7.60 mmol) and diethylaminopyridine (DMAP) (0.09g, 0.76 mmol) were weighed out in a scintillation vial and 5 mL of DCM was added to make a solution. The solution was added to the flask dropwise. After the addition, the mixture was allowed to stir in the water bath overnight. The reaction mixture was filtered to remove dicyclohexylurea and the salts were washed with DCM until white. The filtrate was collected into an evaporating flask and the solvent was removed under reduced pressure. The crude product was isolated by silica gel column chromatography ethyl acetate/ hexanes (v/v, 2/3) as eluent. The eluent was removed by rotary evaporation to yield yellow gel (43.32% yield). 1H NMR (300 MHz, CDCl3, δ, ppm): 4.32 (s, 4H), 3.38 (q, 4H), 2.70 (t, 4H), 2.55 (m, 4H), 1.85 (s, 6H), 1.40 (t, 6H).

2.4. Synthesis of poly(styrene-stat-coumarin methacrylate) (PS-stat-PCMA)

The general procedure for polymerization is as follows: styrene, CMA, diCEP, and AIBN with desired feed ratios were added to a schlenk tube equipped with a magnetic stir bar. Dry DMF was added to the reaction container to dissolve the monomers, chain transfer agent, and the initiator. For example, styrene (1.9 g, 18.26 mmol), CMA (1.3 g, 4.50 mmol), diCEP (0.025 g, 0.043 mmol), and AIBN (1.4 mg, 9.0 μmol) were added with the molar ratios of Styrene:CMA:diCEP:AIBN= 426.8:105.3:1.0:0.2. 3 mL of dry DMF was added to dissolve all

13

the reagents. The flask was then sealed and purged with argon gas for 30 minutes. After purging, an aliquot of 0.2 mL was taken before starting the polymerization at 75 $^{\circ}$C in an oil bath while stirring. After 20 hours, the reaction was stopped by opening the tube to air and quenching it in liquid nitrogen. An aliquot was taken before the work up procedure. The polymer was extracted by precipitating the reaction mixture in methanol and isolated via centrifugation. The precipitation was repeated three times by re-dissolving the polymer in DCM. The complete removal of unreacted monomer was confirmed via NMR and the product was dried in vacuum oven. As SEC instrument (THF) was used to monitor the molecular weight and molecular weight distribution (M_w/M_n) of each polymerization.

2.5. Synthesis of mPEG-PS-stat-PCMA-mPEG

2000 g/mol PEG acrylate was coupled with the hydrophobic block (PS-*stat*-PCMA) via thiol-michael addition reaction. PS-*stat*-PC$_M$A (0.3 g, 15 mmol) and PEG acrylate (3.37 g, 1686 mmol) was added to a 100 mL round bottom flask which was connected to a nitrogen source. Dry THF was added to the flask using a syringe until the polymer was completely dissolved. Then, tributylphosphine (37.01 μl, 607.95 mmol) was added as a catalyst and the reaction was allowed to stir for 15 minutes. Afterwards, hexylamine (19.71 μl, 913.13 mmol) was added to the flask and stirred overnight. The triblock polymer was precipitated in a cold 10:1 mixture of methanol and diethyl ether which was then followed by centrifugation. The procedure was repeated for three times by re-dissolving the polymer in DCM. After confirming the removal of unreacted PEG acrylate via NMR, the triblock polymer was dried in vacuum over for overnight. As SEC instrument (THF) was used to monitor the molecular weight and molecular weight distribution (M_w/M_n) of the polymer.

14

2.6. Synthesis of PDMA-PS-stat-PCMA-PDMA

The reaction was carried out via RAFT polymerization where PS-*stat*-PCMA was treated as the macroCTA. PS-*stat*-PCMA (0.15 g, 0.006 mmol) DMA (0.06 g, 0.60 mmol), and AIBN (0.3 mg, 0.001 mmol) were dissolved in DMF. The mixture was transferred to a Schlenk tube, which was then sealed and purged with argon gas for 30 minutes. An aliquot of 0.2 mL was taken, and the tube was transferred to an oil bath at 75 °C. The reaction was carried out for overnight. Then, the polymerization was stopped by exposing the tube to air and quenching it in liquid nitrogen. The polymer was extracted by precipitating the reaction mixture in methanol three times. The product was dried in a vacuum oven and characterized via NMR and DMF SEC.

2.7. Synthesis of PNaSS-PS-stat-PCMA-PNaSS

The reaction was carried out via aqueous RAFT polymerization. PS-*stat*-PCMA (0.4 g, 0.013 mmol), and AIBN (0.4 mg, 0.003 mmol) were dissolved in DMF. NaSS (0.2 g, 0.970 mmol) was dissolved in D_2O. Both DMF solution and D_2O solution were then transferred into a Schlenk tube. The tube was sealed and purged with argon gas for 30 minutes. After purging, an aliquot of 0.2 mL was taken before starting the polymerization at 65 °C in an oil bath for 1 hour. The triblock polymer was obtained as a precipitate in the mixture of DMF and D_2O, which was then decanted off to characterize. The polymer was dried in a vacuum oven and was characterized via NMR and DMF SEC.

2.8. Synthesis of PDMAPS-PS-stat-PCMA-PDMAPS

The reaction was carried out via RAFT polymerization where PS-*stat*-PCMA was treated as the macroCTA. PS-*stat*-PCMA (0.3 g, 0.012 mmol), AIBN (0.25 µg, 0.002 mmol), and

DMAPS (0.2 g, 0.71 mmol) were dissolved in hexafluoroisopropanol. The solution mixture was transferred to a schlenk tube equipped with a stir bar, which was then sealed and purged with argon gas for 30 minutes. The reaction tube was then transferred to an oil bath at 65 $^{\circ}$C. The polymerization was stopped after 17 hours by opening the tube to air and quenching the reaction with liquid nitrogen. The reaction mixture was then dialyzed against deionized water to ensure the removal of unreacted monomer. The polymer was characterized via NMR and HFIP SEC .

2.9. Preparation of vesicles

The vesicles, along with other assembled morphologies, were obtained by the self-assembly and co-assembly of the triblock polymers via solvent displacement technique. The general procedure is as follows: 5 mg of the triblock polymer (either one species or a mixture of two) was dissolved in 1 mL of a 4:1 mixture of THF:dioxane. Deionized water (1 mL) was added to the vial with a syringe pump while stirring. A cloudy suspension was observed after the addition of about 20% of deionized water.

2.10. Characterization of vesicles
2.10.1. Dynamic and static light scattering

Dynamic light scattering and static light scattering data were collected using incident light at 633 nm from a Research Electro Optics HeNe laser operating at 40 mW. Brookhaven Instruments BI-200SM goniometer was used to measure the time-dependent scattering intensities at angles 45, 60, 75, 90, 105, and 120°. The system was equipped with an avalanche photodiode detector and TurboCorr correlator. The light scattering experiments were done at 25 $^{\circ}$C. The decay rate was obtained from the quadratic fit of the autocorrelation function ($g^2(\tau)$), where τ is

the relaxation time. The apparent diffusion coefficient was obtained by plotting Γ versus q^2, where q is the wave vector and Γ is the relaxation frequency.

$$\Gamma = 1/\tau$$

$$q = \frac{4\pi n}{\lambda}\sin(\theta/2)$$

where, λ is the wavelength of the incident light, θ is the scattering angle, and n is the refractive index of the solvent. Using the Stokes-Einstein equation, the hydrodynamic radius (R_h) was calculated.

$$D_{app} = \frac{k_B T}{6\pi\eta R_h}$$

where, k_B is the Boltzmann's constant and η is the viscosity of solvent.

The hydrodynamic radius was doubled to get the hydrodynamic diameter of the particles, which are reported as the DLS data.

Angular dependent static light scattering experiments were carried out to determine the radius of gyration (R_g) of the assembled morphologies. The scattering intensities were measured as a function of scattering angles 45, 50, 60, 70, 80, 90, 105, 115, 120, and 140°. R_g was obtained from the Zimm plot of scattering intensity versus square of scattering vector.

2.10.2. Transmission Electron Microscopy (TEM)

TEM was performed on a JEM-1400 microscope at an acceleration voltage of 40-120 kV. The sample was prepared by placing the drop of the solution on a carbon-coated copper grid. TEM imaging was done at the Shared Instrumentation Facility at Louisiana State University.

Chapter 3

Results and Discussion

To study the assembly behavior of linear amphiphilic triblocks during the fabrication of polymer vesicles, we synthesized four different triblock copolymers. We synthesized two neutral, one zwitterionic, and one anionic triblocks in order to analyze the influence of hydrophobic interaction and electrostatic interaction during the assembly. All four triblocks contain the same composition of hydrophobic block in the center, which is obtained by the co-polymerization of styrene and CMA via RAFT (Scheme 3). Among the two neutral triblocks, one contains PEG as its hydrophilic block and the other contains PDMA as its hydrophilic block. The hydrophilic blocks in the anionic triblock and the zwitterionic triblock are composed of PNaSS and DMAPS respectively. All four triblocks were self-assembled. In addition, we co-assembled the two neutral triblocks in different ratios to understand their interaction in vesicle fabrication during co-assembly.

### 3.1. Synthesis of monomer 7-(2-hydroxyethoxy)-4-methylcoumarin (CMA)

7-(2- Hydroxyethoxy)-4-methylcoumarin was first synthesized via the Williamson ether synthesis mechanism, which was confirmed by the presence of doublets at 3.73 ppm and a triplet at 4.08 ppm in ^{1}H NMR (Figure A1). The ether was then reacted with methacryloyl chloride to obtain CMA. The formation of the ester linkage, and thus the synthesis of CMA, was confirmed by the presence of a singlet at 1.96 ppm and another singlet at 6.15 ppm in ^{1}H NMR (Figure A2).
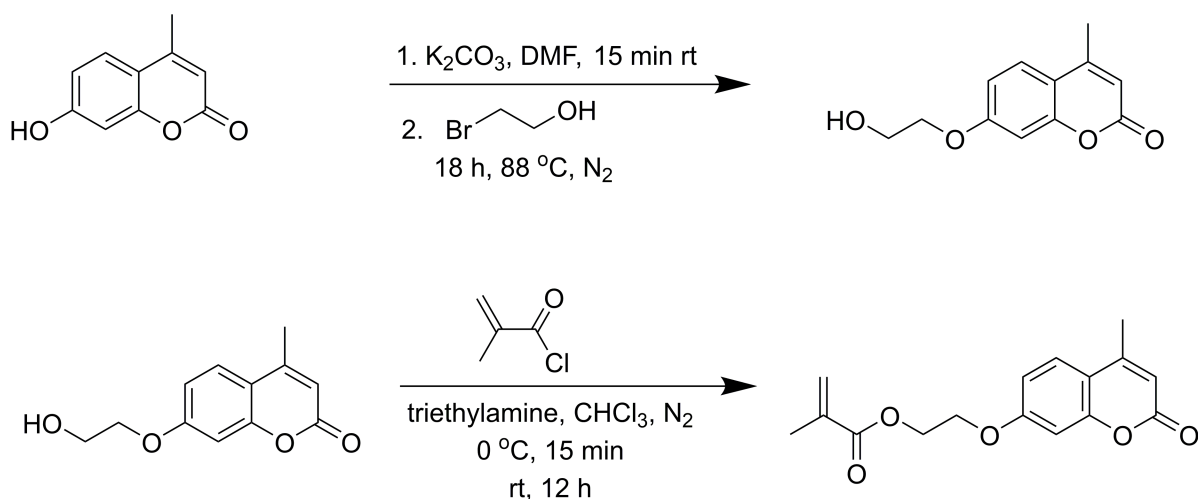
Scheme 1. Synthesis of monomer, CMA

3.2. Synthesis of *di*-4-cyano-4-(ethylsulfanylthiocarbonyl)sulfanylpentanoic acid diCEP

A di-functional chain transfer agent was chosen in order to impart functionality on both

ends of the polymer. First, the monofunctional chain transfer agent, CEP, was successfully

synthesized (Figure A3). Then, CEP was coupled to obtain diCEP via a Steglich esterification.

The presence of a singlet at 4.32 ppm in ^{1}H-NMR confirmed the synthesis of diCEP (Figure A4).
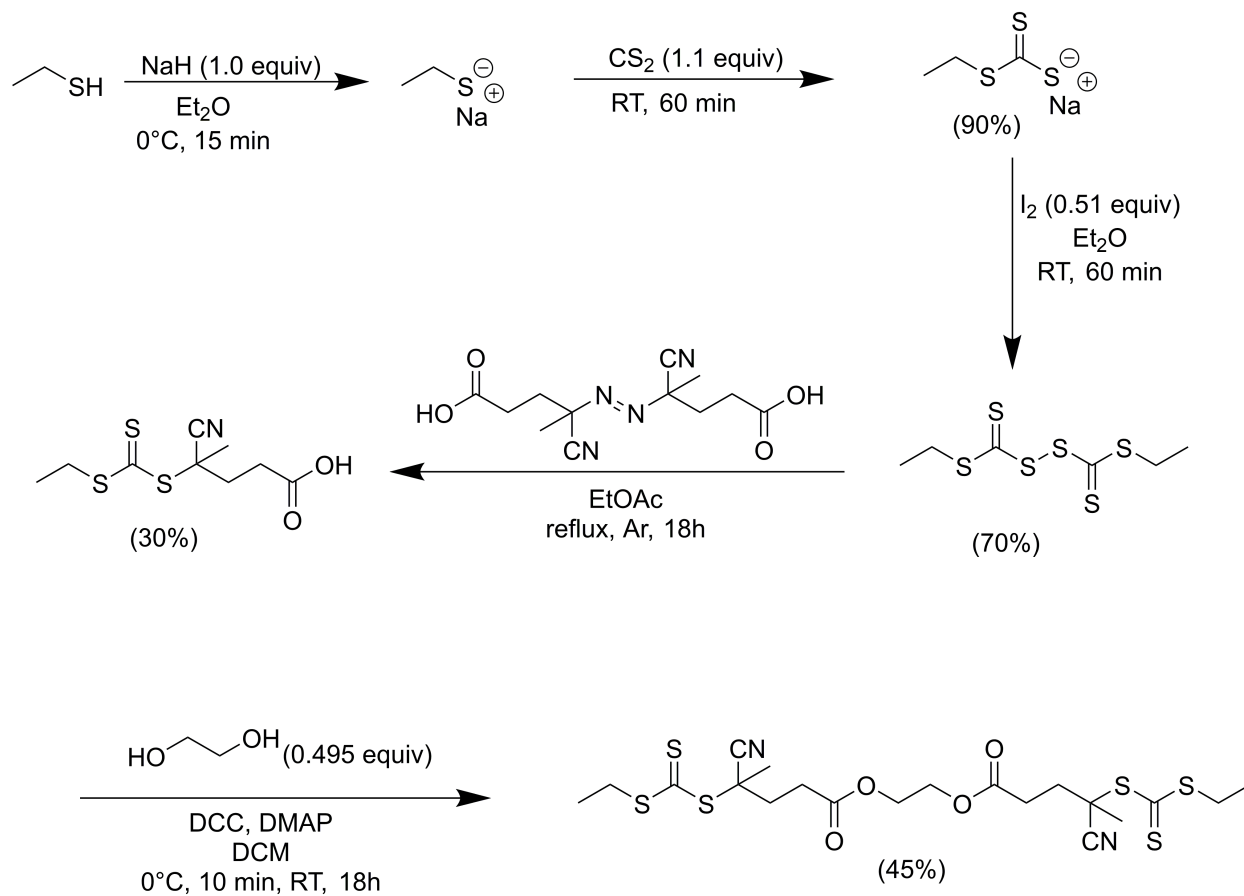
Scheme 2. Synthesis of RAFT chain transfer agent, diCEP

3.3. Synthesis of PS-*stat*-PCMA
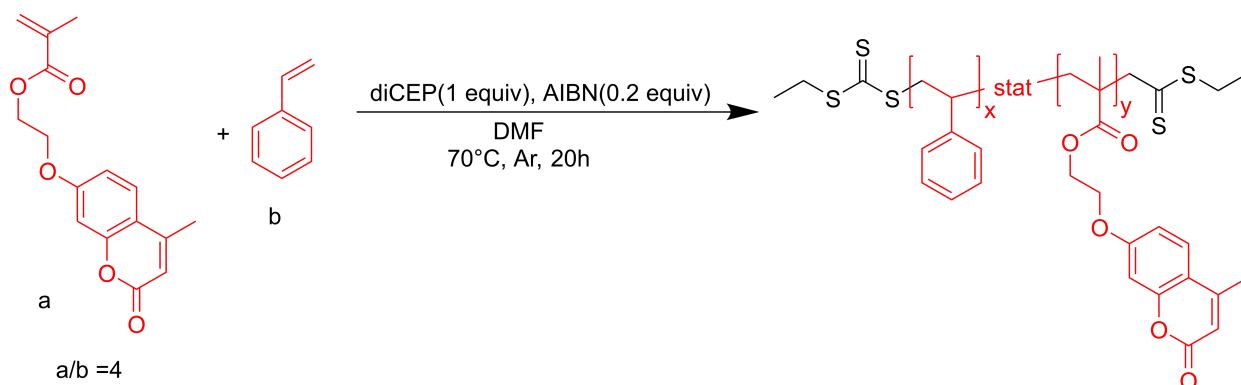
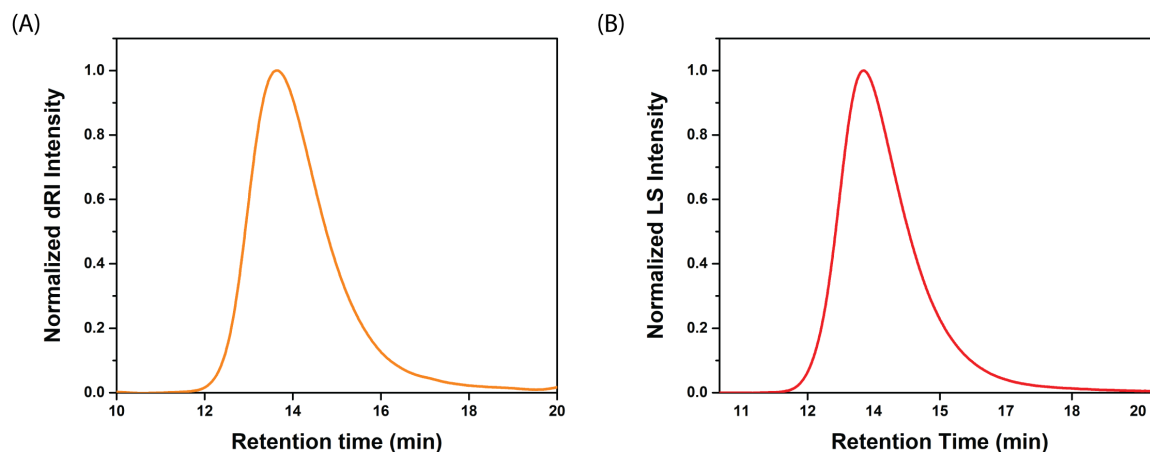

Scheme 3. RAFT polymerization of styrene and CMA

Figure 3. Size exclusion chromatography, (A)-light scattering and (B)-differential refractive index plots of PS-*stat*-PCMA
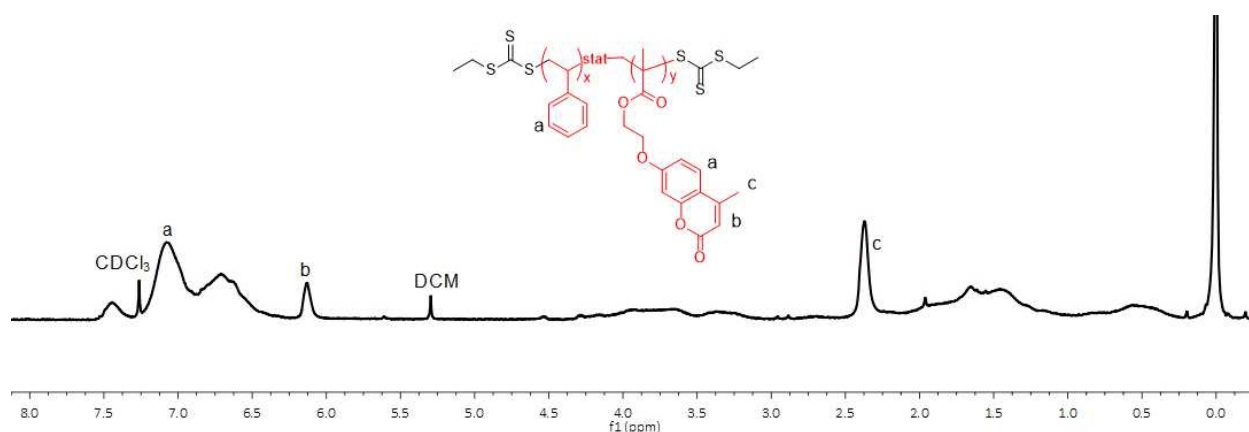

Figure 4. ^{1}H-NMR of PS-*stat*-PCMA

PS-*stat*-PCMA was successfully synthesized as shown by size exclusion chromatography and ^{1}HNMR in Figure 3 and Figure 4 respectively. The conversion of the reaction was 30%. At 30% conversion, the theoretical and the experimental molecular weights of the polymer was 25,404 g/mol and 25,800 g/mol respectively. The dispersity of the polymer was 1.17.

3.4. Synthesis of neutral triblocks

3.4.1. mPEG-PS-*stat*-PCMA-mPEG
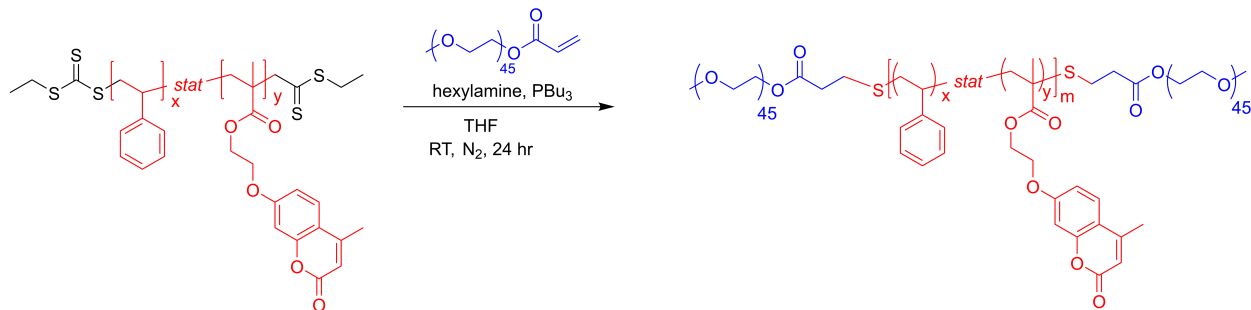
Scheme 4. Thio-michael reaction for the coupling of mPEG with PS-*stat*-PCMA
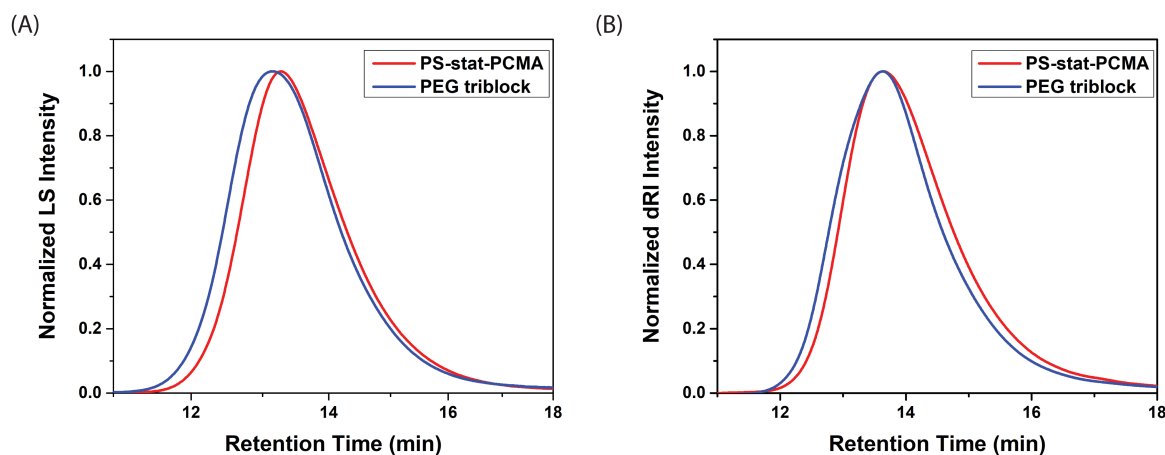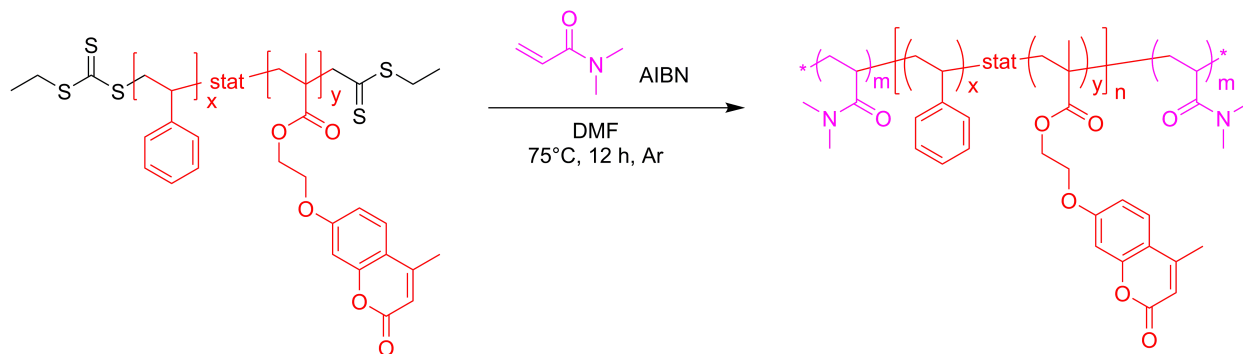

Figure 5: Decrease in retention time observed via size exclusion chromatography, (A)-light scattering and (B)- differential refractive index for the synthesis of PEG triblock from PS-*stat*-PCMA

The synthesis of mPEG-*b*-PS-*stat*-PCMA-*b*-mPEG was confirmed by the presence of a peak at 3.64 ppm in ^{1}H NMR **(Figure A5)** and size exclusion chromatography. The molecular weight of the triblock was 33,500 g/mol from SEC. From ^{1}H NMR integration, 8H contributed to the peak at 3.64 ppm (representing PEG) and 1H contributed to the peak at 6.13 ppm (representing CMA). Thus, it was confirmed that there were two PEG blocks, each 2000 g/mol, per hydrophobic block in the triblock. Therefore, the triblock contained 13% hydrophilic content and 87% hydrophobic content.

3.4.2. PDMA-PS-*stat*-PCMA-PDMA

Scheme 5. Chain extension of PS-*stat*-PCMA with dimethylacrylamide
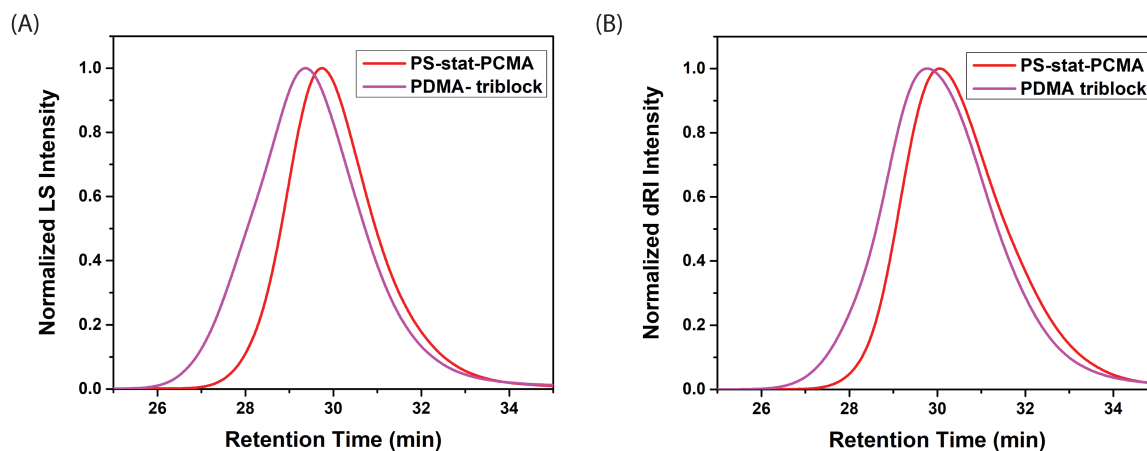

Figure 6: Decrease in retention time observed via size exclusion chromatography, (A)-light scattering and (B)- differential refractive index for the synthesis of PDMA triblock from PS-*stat*-PCMA

The synthesis of PDMA-PS-*stat*-PCMA-PDMA was confirmed by the presence of a peak at 2.91 ppm in ^{1}H NMR which represent the methyl peaks in DMA **(Figure A6)**. Also, size exclusion chromatography showed a decrease in retention time as compared to the hydrophobic block. The molecular weight of the triblock was 29,292 g/mol. The triblock contained 15% hydrophilic content and 85% hydrophobic content.

Characterization of the vesicles obtained from neutral triblocks

Table 1. Size characterization of morphologies from neutral triblock assemblies in water via light scattering

Polymer composition	Radius of gyration $(R_g)^a$ (nm)	Hydrodynamic radius $(R_h)^b$ (at 90°) (nm)	R_g/R_h
PEG-PS-*stat*-pCMA-PEG	67.5	62.2	1.085
DMA-PS-*stat*-pCMA-DMA	229.5	180.4	1.272
PEG triblock and DMA triblock (50:50)	35.5	38.2	0.929
PEG triblock and DMA triblock (80:20)	43.1	38.5	1.119
PEG triblock and DMA triblock (20:80)	50.3	48.3	1.041

The triblocks were assembled by the addition of deionized water in the solution of polymer with organic solvent. [a] R_g was determined from the Zimm plot of scattering intensity versus square of scattering vector, which was obtained from the static light scattering. [b] R_h was obtained from the dynamic light scattering.

TEM Results

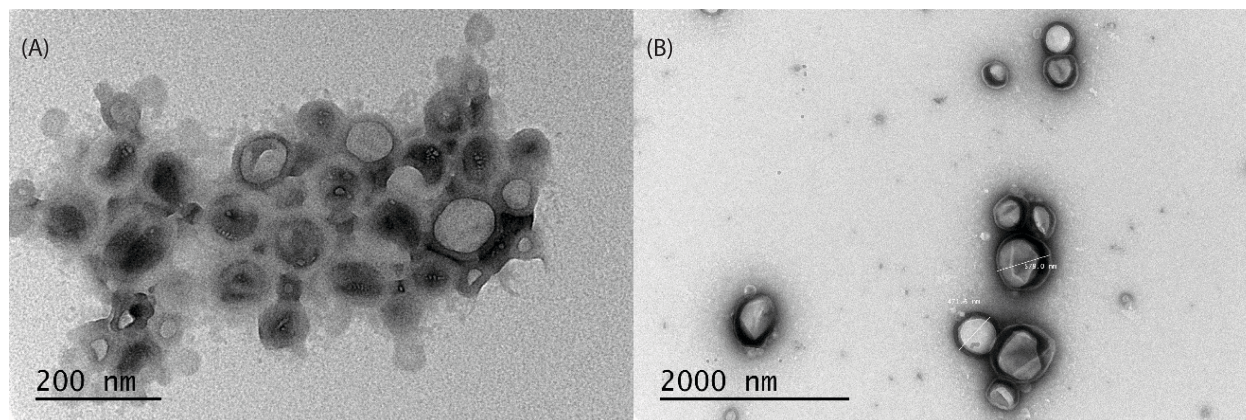**Self-assembly of the triblocks**

Figure 7. Morphologies from the self-assembly of (a) PEG triblock and (b) DMA triblock
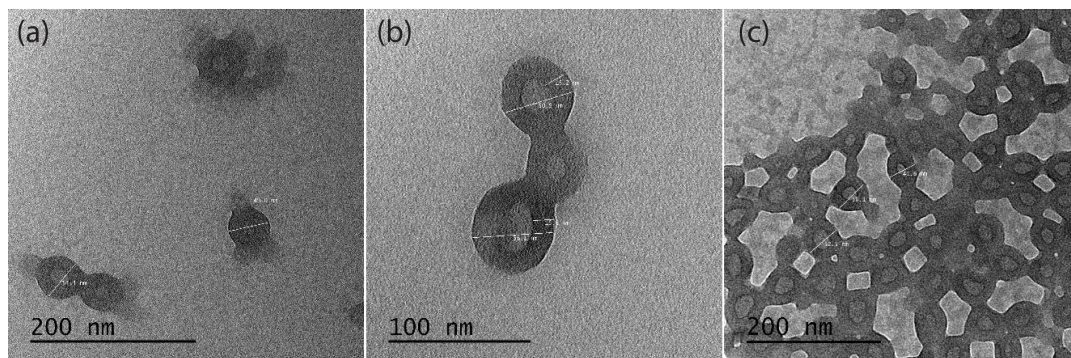
Co-assembly of the triblocks

Figure 8. Morphologies from the co-assembly of (a) 50:50 (b) 80:20 and (c) 20:80 ratio of PEG triblock and DMA triblock

Dynamic and static light scattering experiments were performed on the assembled morphologies to study their sizes based on the hydrodynamic radius and radius of gyration values. Also, the value of R_g/R_h was used to analyze the type of the morphology in the sample. According to the literature, the value of R_g/R_h is expected to be 1 for vesicles, less than 1 for spherical micelles, and greater than 1 for cylindrical micelles[20]. The R_g/R_h value for the self-

assembly of the DMA triblock indicated the formation of cylindrical micelles instead of vesicles, since the ratio is larger than 1. As observed from both light scattering and TEM data, the self-assembly of the triblocks led to the fabrication of larger morphologies as compared to those obtained from the co-assembly of the triblocks. The average radii of the morphologies obtained from the self-assembly of the PEG triblocks and DMA triblocks was about 65 nm (Figure 7a) and 200 nm (Figure 7b) respectively.

The radii of the morphologies obtained from the co-assembly of the triblocks ranged from 35 nm to 50 nm. Based on the TEM images, it was confirmed that both the self-assembly and the co-assembly of the triblocks led to the fabrication of vesicles. However, self-assembly of the triblocks also led to some other morphologies such as micelles, and large compound micelles (Figure 7a). Also, based on the TEM results, the co-assembly of the triblocks resulted in more uniform distribution of morphologies, in terms of sizes and shapes, as compared to those obtained from the self-assembly of the triblocks. From this, it was understood that the segregation of the hydrophilic blocks towards the core versus the corona of the vesicles was favored as a result of the co-assembly of the triblocks. The interfacial energy of the vesicles obtained from the co-assembly of the triblocks was strongly size-dependent, thus leading to the formation of smaller structures with a uniform distribution. Moreover, there was a single distribution of the morphologies, based on both the light scattering and the TEM data, which indicated that the triblocks co-assembled. In addition, the approximate sizes of the vesicles as observed from the TEM images corresponded to that obtained from the light scattering experiments. Since the TEM images were captured three days later than the light scattering experiments, retention of the sizes indicated that the structures were frozen and maintained their integrity in the aqueous solvent. The vesicles did not undergo fusion or fission phenomena.

26

3.5. Charged triblocks

3.5.1. Synthesis of PNaSS-PS-*stat*-PCMA-PNaSS

Scheme 6. Chain extension of PS-*stat*-PCMA with NaSS
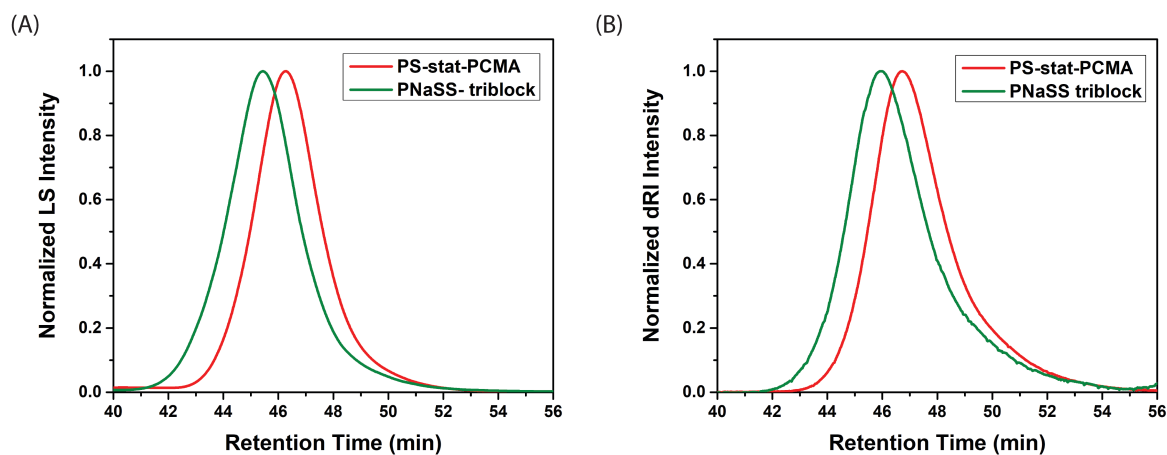

Figure 9: Decrease in retention time observed via size exclusion chromatography, (A)-light scattering and (B)- differential refractive index for the synthesis of PNaSS triblock from PS-*stat*-PCMA

PNaSS-PS-*stat*-PCMA-PNaSS was synthesized successfully. The retention time of the triblock was lower as compared to that of the hydrophobic block as observed from the SEC data. Since the peaks from the NaSS group overlap with that of styrene from the hydrophobic block, it was difficult to characterize the triblock by the appereance of a certain peak. However, as the

polymer had precipitated at the end of the reaction and was decanted off of the solution of DMF and deionized water, the absence of NaSS monomer in the reaction solution confirmed the chain extension polymerization (**Figure A8 and Figure A9**). Since there was no monomer left in the reaction solution, it indicated that the chain extension reaction underwent 100% conversion. The molecular weight of the triblock was 36,000 g/mol via SEC. The triblock contained 17% hydrophilic content and 83% hydrophobic content.

3.5.2. Synthesis of PDMAPS-PS-*stat*-PCMA-PDMAPS
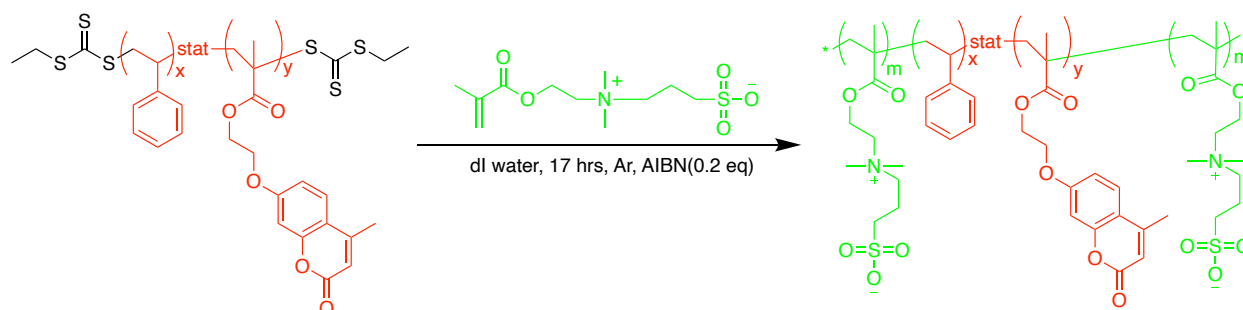
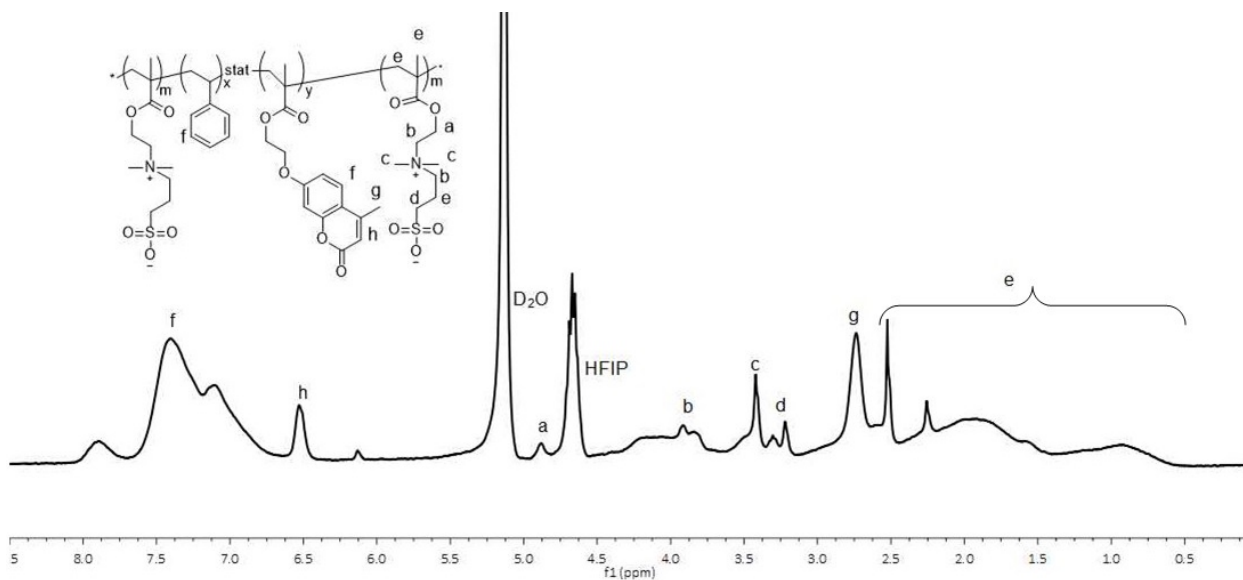**Scheme 7**. Chain extension of PS-*stat*-PCMA with DMAPS

Figure 10. NMR of PDMAPS-PS-*stat*-PCMA-PDMAPS

28

Characterization of vesicles obtained from charged triblocks

Table 2. Size characterization of morphologies from ionic triblock assemblies in water via light scattering

Polymer composition	Radius of gyration $(R_g)^a$ (nm)	Hydrodynamic radius $(R_h)^b$ (at 90°) (nm)	R_g/R_h
NaSS-PS-*stat*-pCMA-NaSS	481.03	189.35	2.54
DMAPS-PS-*stat*-pCMA-DMAPS	194.5	190.4	1.021

The triblocks were assembled by the addition of deionized water in the solution of polymer with organic solvent. ^{a} R_g was determined from the Zimm plot of scattering intensity versus square of scattering vector, which was obtained from the static light scattering. ^{b} R_h was obtained from the dynamic light scattering at 90° goniometer angle.

TEM Results

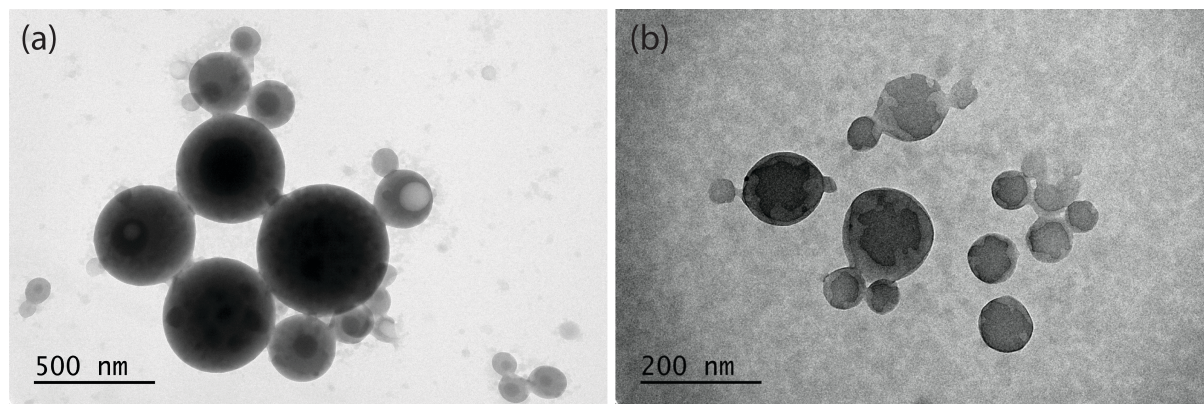**Self-assembly of the triblocks**

Figure 11. Morphologies from the self-assembly of (a) NaSS triblock and (b) DMAPS triblock

Dynamic and static light scattering experiments were performed to analyze the sizes of the morphologies. Moreover, TEM images were captured to study the shapes and distribution of the assembled morphologies. The self-assembly of the anionic (Figure 11a) and zwitterionic (Figure 11b) triblocks did not result in the fabrication of vesicles. The self-assembly of anionic triblocks showed the formation of large compound micelles. In the assembly of amphiphilic block copolymer, such behavior is observed due to the higher content of hydrophobic block as compared to the hydrophilic content as required for the fabrication of vesicles. Therefore, in future, it would be beneficial to study the assembly behavior of the anionic and zwitterionic triblocks by increasing their hydrophilic content. The self-assembly of zwitterionic triblocks resulted in structures with irregular membranes. In general, as microphase separation occurs, the blocks arrange themselves in such a way that the total interfacial energy is minimized and thus they form smooth membranes. The assembly of the zwitterionic triblocks might have resulted in the formation of irregular micelles which are indicative of solid precipitates. In future, we plan on conducting the assembly of the zwitterionic triblocks by the addition of salt which might help in the formation of the coacervates. The addition of salt can help to increase the solubility of the zwitterionic polymers by screening the inter- and intrachain attraction of opposite charges in the zwitterionic polymers.[17] On the addition of salt, the ionic repulsion between the charges gets reduced and the attractive inter- and intramolecular forces dominate.[17]

Chapter 4

Conclusion and Future Directions

A series of amphiphilic triblock copolymers were synthesized. As determined by DLS, SLS, and TEM, the neutral triblocks were self- and co-assembled into polymer vesicles. The co-assembly of the PEG triblock and DMA triblock resulted in smaller vesicles as compared to the ones obtained from the self-assembly. No significant difference was observed, in terms of size and morphology, when the two triblocks were co-assembled in different ratios. However, the self-assembly of neutral triblocks led to the formation of other morphologies such as micelles and large compound micelles in addition to vesicles. Future work is needed to further understand the membrane composition of the vesicles obtained from the co-assembly of the triblocks. Fluorescence microscopy can be used to distinguish a certain type of triblock with fluorescence tag in the membrane. Moreover, fourier transformation of TEM images can be done to obtain phase contrast images, which will help to understand the presence of different triblocks in the membrane.[38] In addition, atomic force microscopy can be utilized to study the difference in the moduli of the membrane. Previously, some work had been done in the fabrication of giant unilamellar vesicles via electroformation. Thus, the work can be expanded by the fabrication of giant unilamellar vesicles to study the assembly behavior at macroscale size range.

The self-assembly of the zwitterionic as well as the anionic triblock did not form vesicles. It might be due to the higher content of hydrophobic block as compared to the hydrophilic blocks. Due to time constraint, the co-assembly of the ionic triblocks was not conducted. In future, it is desired to self- and co-assemble zwitterionic and anionic triblocks by varying the composition ratio of hydrophobic and hydrophilic blocks. In addition, the self- and co-assembly

of zwitterionic and anionic triblocks will be conducted in salt solution which might aid in the

assembly of triblocks.

References

(1)   Zhu, Y.; Yang, B.; Chen, S.; Du, J. Polymer Vesicles: Mechanism, Preparation, Application, and Responsive Behavior. *Prog. Polym. Sci.* **2017**, *64* (June), 1–22.

(2)   Zhu, Y.; Fan, L.; Yang, B.; Du, J. Multifunctional Homopolymer Vesicles for Facile Immobilization of Gold Nanoparticles and Effective Water Remediation. *ACS Nano* **2014**, *8* (5), 5022–5031.

(3)   Geng, Q.; Xiao, J.; Yang, B.; Wang, T.; Du, J. Rationally Engineering Dual Missions in One Statistical Copolymer Nanocapsule: Bacterial Inhibition and Polycyclic Aromatic Hydrocarbon Capturing. *ACS Macro Lett.* **2015**, *4* (5), 511–515.

(4)   Hu, J.; Koleva, D. A.; Petrov, P.; van Breugel, K. Polymeric Vesicles for Corrosion Control in Reinforced Mortar: Electrochemical Behavior, Steel Surface Analysis and Bulk Matrix Properties. *Corros. Sci.* **2012**, *65*, 414–430.

(5)   Berthier, D. L.; Schmidt, I.; Fieber, W.; Schatz, C.; Furrer, A.; Wong, K.; Lecommandoux, S. Controlled Release of Volatile Fragrance Molecules from PEO-b-PPO-b-PEO Block Copolymer Micelles in Ethanol-Water Mixtures. *Langmuir* **2010**, *26* (11), 7953–7961.

(6)   Mai, Y.; Eisenberg, A. Self-Assembly of Block Copolymers. *Chem. Soc. Rev.* **2012**, *41* (18), 5969–5985.

(7)   Zhao, Y.; Li, X.; Zhao, X.; Yang, Y.; Li, H.; Zhou, X.; Yuan, W. Asymmetrical Polymer Vesicles for Drug Delivery and Other Applications. *Front. Pharmacol.* **2017**, *8*, 1–9.

(8)   Brinkhuis, R. P.; Rutjes, F. P. J. T.; Van Hest, J. C. M. Polymeric Vesicles in Biomedical Applications. *Polym. Chem.* **2011**, *2* (7), 1449–1462.

(9)   Feng, H.; Lu, X.; Wang, W.; Kang, N. G.; Mays, J. W. Block Copolymers: Synthesis,

Self-Assembly, and Applications. *Polymers (Basel).* **2017**, *9* (10).

(10)   Lodge, T. P. Block Copolymer: Past Successs and Future Challenges. *Macromol. Chem. Phys.* **2003**, 204, 265–273.

(11)   Matsen, M. W.; Bates, F. S. Origins of Complex Self-Assembly in Block Copolymers. *Macromolecules* **1996**, *29* (23), 7641–7644.

(12)   Sugiyama, K. Block Copolymer Synthesis. *Encycl. Polym. Nanomater.* **2014**, *4* (1999), 1–10.

(13)   Chiefari, J.; Chong, Y. K. B.; Ercole, F.; Krstina, J.; Jeffery, J.; Le, T. P. T.; Mayadunne, R. T. A.; Meijs, G. F.; Moad, C. L.; Moad, G.; et al. Living Free-Radical Polymerization by Reversible Addition - Fragmentation Chain Transfer : The RAFT Process *Maromolecules*. **1998**, *9297* (98), 5559–5562.

(14)   Laschewsky, A. Structures and Synthesis of Zwitterionic Polymers. *Polymers.* **2014**, 6, 1544–1601.

(15)   Maddikeri, R. R.; Colak, S.; Gido, S. P.; Tew, G. N. Zwitterionic Polymersomes in an Ionic Liquid : Room Temperature TEM characterization. *Biomacromolecules* **2011**, 8–13.

(16)   Bengani, P.; Kou, Y.; Asatekin, A. Zwitterionic Copolymer Self-Assembly for Fouling Resistant , High Fl Ux Membranes with Size-Based Small Molecule Selectivity. *J. Membr. Sci*. **2015**, *493*, 755–765.

(17)   Blackman, L. D.; Gunatillake, P. A.; Cass, P.; Locock, K. E. S. An introduction to zwitterionic polymer behavior and applications in solution and at surfaces. *Chem. Soc. Rev.* **201**9, 48, 757-770.

(18)   Liu, Y.; Fan, B.; Shi, Q.; Dong, D.; Gong, S.; Zhu, B.; Fu, R.; Thang, S. H.; Cheng, W. Covalent-Cross-Linked Plasmene Nanosheets. *ACS Nano* **2019**, *13* (6), 6760–6769.

(19)   Onbulak, S.; Rzayev, J. Cylindrical Nanocapsules from Photo-Cross-Linkable Core-Shell
        Bottlebrush Copolymers. *Polym. Chem.* **2015**, *6* (5), 764–771.

(20)   Patterson, J. P.; Robin, M. P.; Chassenieux, C.; Colombani, O.; Reilly, R. K. O. The
        analysis of solution self-assembled polymeric nanomaterials. *Chem Soc Rev*. **2014**, 43,
        2412-2425.

(21)   Van Hest, J. C. M., Delnoye, D. A. P., Baars, M. W. P. L., van Genderen, M. H. P., &
        Meijer, E. W. Polystyrene-Dendrimer Amphiphilic Block Copolymers with a Generation-
        Dependent Aggregation. *Science*. **1995**, *268*, 1592–1595.

(22)   Chidanguro, T.; Ghimire, E.; Liu, C. H.; Simon, Y. C. Polymersomes: Breaking the Glass
        Ceiling? *Small* **2018**, *14* (46), 1–17.

(23)   Perrier, S. 50th Anniversary Perspective: RAFT Polymerization - A User Guide.
        Macromolecules **2017**, *50* (19), 7433–7447.

(24)   Darling, S. B. Directing the Self-Assembly of Block Copolymers. *Prog. Polym. Sci.* **2007**,
        32 (10), 1152–1204.

(25)   Blanazs, A.; Armes, S. P.; Ryan, A. J. Self-Assembled Block Copolymer Aggregates:
        From Micelles to Vesicles and Their Biological Applications. *Macromol. Rapid Commun.*
        2009, *30* (4–5), 267–277.

(26)   Wischerhoff, E.; Badi, N.; Laschewsky, A.; Lutz, J.-F. Smart Polymer Surfaces:
        Concepts and Applications in Biosciences. *Adv. Polym. Sci*. **2010**, 240(1), 1–33.

(27)   Du, J.; Armes, S. P. Preparation of Biocompatible Zwitterionic Block Copolymer
        Vesicles by Direct Dissolution in Water and Subsequent Silicification within Their
        Membranes. *Langmuir* **2009**, *25* (16), 9564–9570.

(28)   Schulz, M.; Olubummo, A.; Binder, W. H. Beyond the Lipid-Bilayer: Interaction of Polymers and Nanoparticles with Membranes. *Soft Matter* **2012**, *8* (18), 4849–4864.

(29)   Cai, Y.; Armes, S. P. A Zwitterionic ABC Triblock Copolymer That Forms a "Trinity" of Micellar Aggregates in Aqueous Solution. *Macromolecules* **2004**, *37* (19), 7116–7122.

(30)   Lebègue, E.; Farre, C.; Jose, C.; Saulnier, J.; Lagarde, F.; Chevalier, Y.; Chaix, C.; Jaffrezic-Renault, N. Responsive Polydiacetylene Vesicles for Biosensing Microorganisms. *Sensors (Switzerland)* **2018**, *18* (2), 1–16.

(31)   Leong, J.; Teo, J. Y.; Aakalu, V. K.; Yang, Y. Y.; Kong, H. Engineering Polymersomes for Diagnostics and Therapy. *Adv. Healthc. Mater.* **2018**, *7* (8), 1–27.

(32)   Matyjaszewski, K. Atom Transfer Radical Polymerization (ATRP): Current Status and Future Perspectives. *Macromolecules* **2012**, *45* (10), 4015–4039.

(33)   Nicolas, J.; Guillaneuf, Y.; Lefay, C.; Bertin, D.; Gigmes, D.; Charleux, B. Nitroxide-Mediated Polymerization. *Prog. Polym. Sci.* **2013**, *38* (1), 63–235.

(34)   Li, C.; Tho, C. C.; Galaktionova, D.; Chen, X.; Král, P.; Mirsaidov, U. Dynamics of Amphiphilic Block Copolymers in an Aqueous Solution: Direct Imaging of Micelle Formation and Nanoparticle Encapsulation. *Nanoscale* **2019**, *11* (5), 2299–2305.

(35)   Ge, Z.; Liu, S. Supramolecular Self-Assembly of Nonlinear Amphiphilic and Double Hydrophilic Block Copolymers in Aqueous Solutions. *Macromol. Rapid Commun.* **2009**, *30* (18), 1523–1532.

(36)   Lodge, T. P.; Bang, J.; Li, Z.; Hillmyer, M. A.; Talmon, Y. Strategies for Controlling Intra- and Intermicellar Packing in Block Copolymer Solutions: Illustrating the Flexibility of the Self-Assembly Toolbox. *Faraday Discuss.* **2005**, *128*, 1–12.

(37) Palivan, C. G.; Goers, R.; Najer, A.; Zhang, X.; Car, A.; Meier, W. Bioinspired Polymer

Vesicles and Membranes for Biological and Medical Applications. *Chem. Soc. Rev.* **2016**,

45 (2), 377–411.

(38) Zhu, Y.; Wang, F.; Zhang, C.; Du, J. Preparation and Mechanism Insight of Nuclear

Envelope-like Polymer Vesicles for Facile Loading of Biomacromolecules and Enhanced

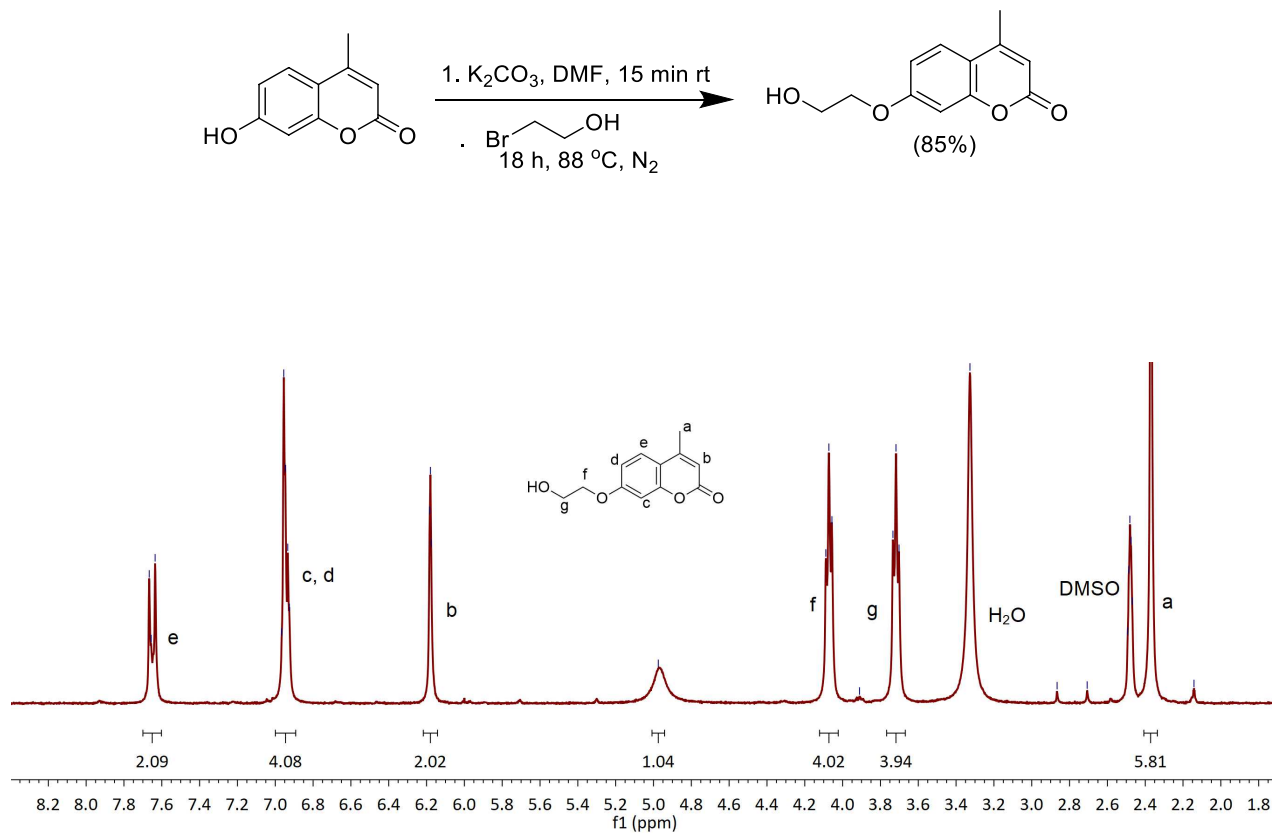Biocatalytic Activity. *ACS Nano* **2014**, *8* (7), 6644–6654.

Synthesis of CMA

Step 1:

Figure A1. Synthesis of 7-(2- Hydroxyethoxy)-4-methylcoumarin

Step 2:
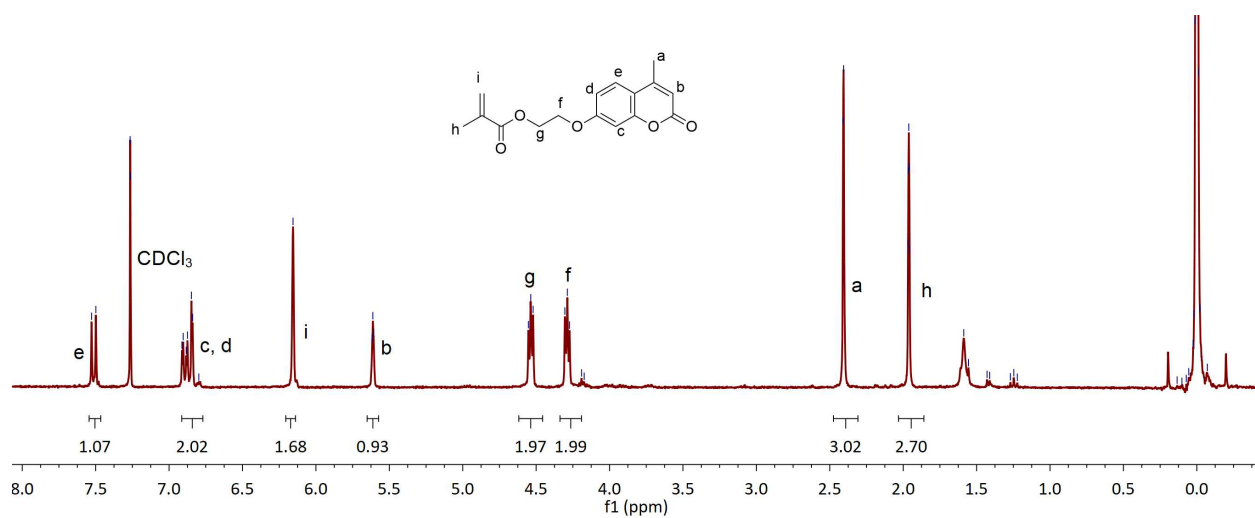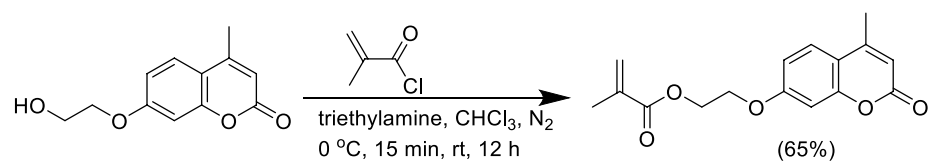
Figure A2. Synthesis of CMA

Synthesis of diCEP

Step 1:
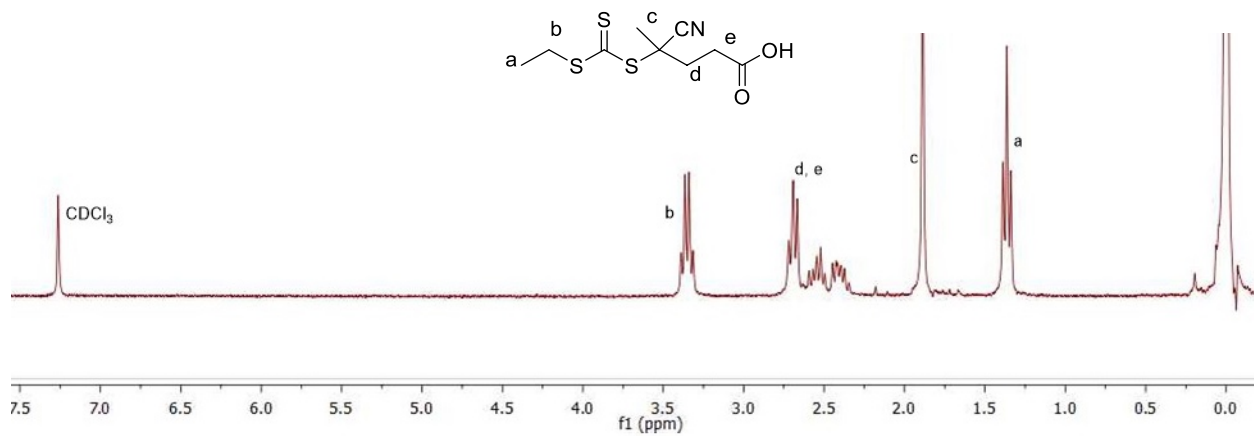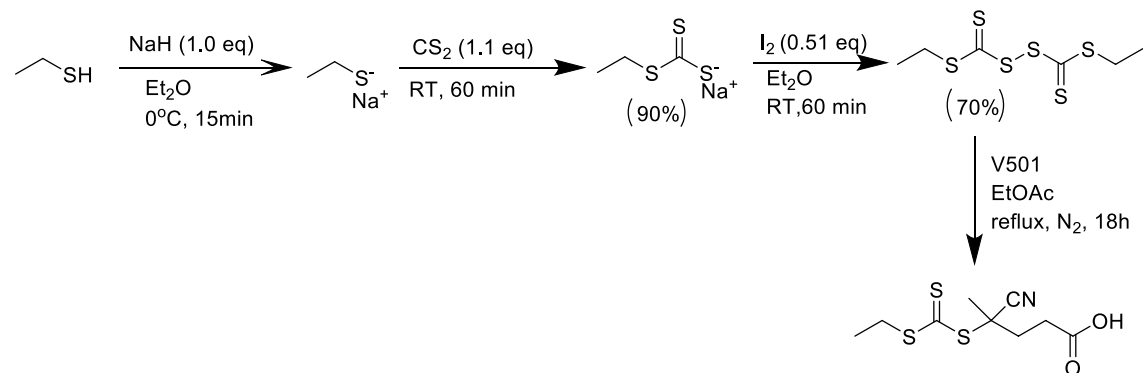
Figure A3. Synthesis of CEP

Step 2:
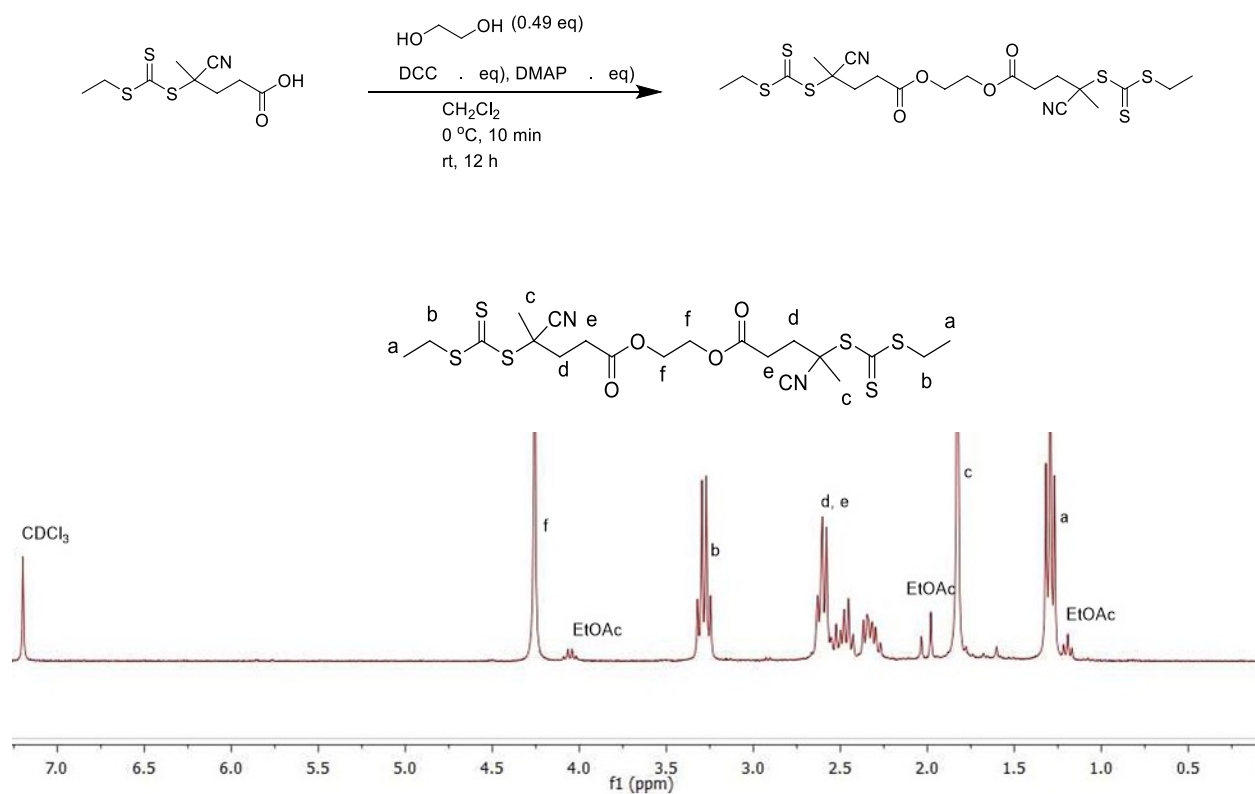
Figure A4. Synthesis of diCEP
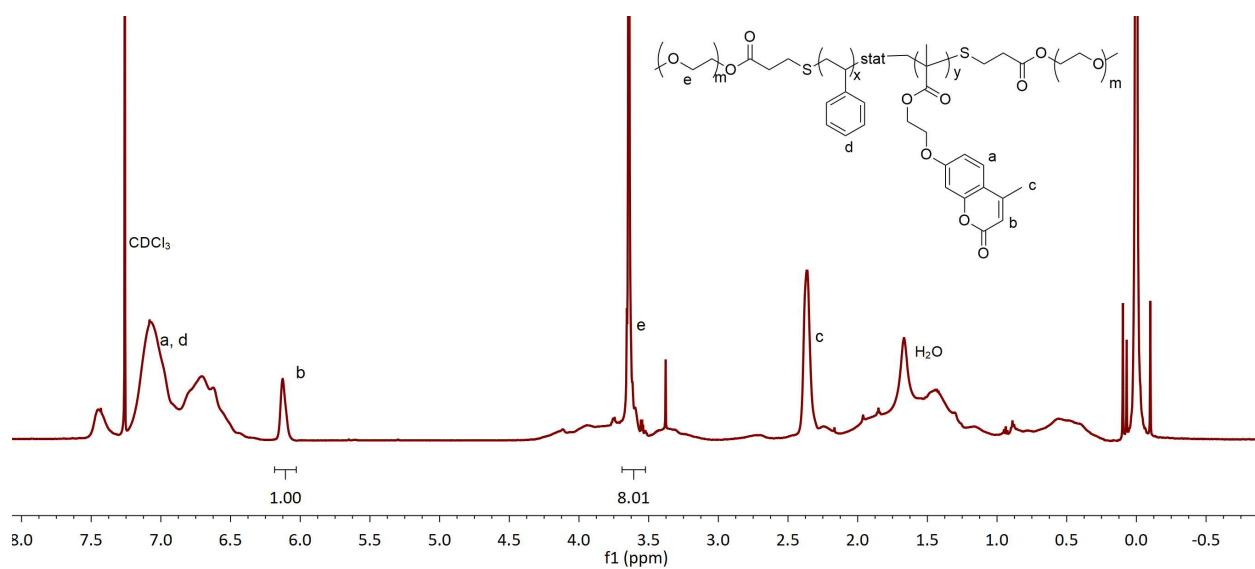
41

NMR Analysis of PEG-PS-*stat*-PCMA-PEG

Figure A5. NMR of PEG-PS-*stat*-PCMA-PEG
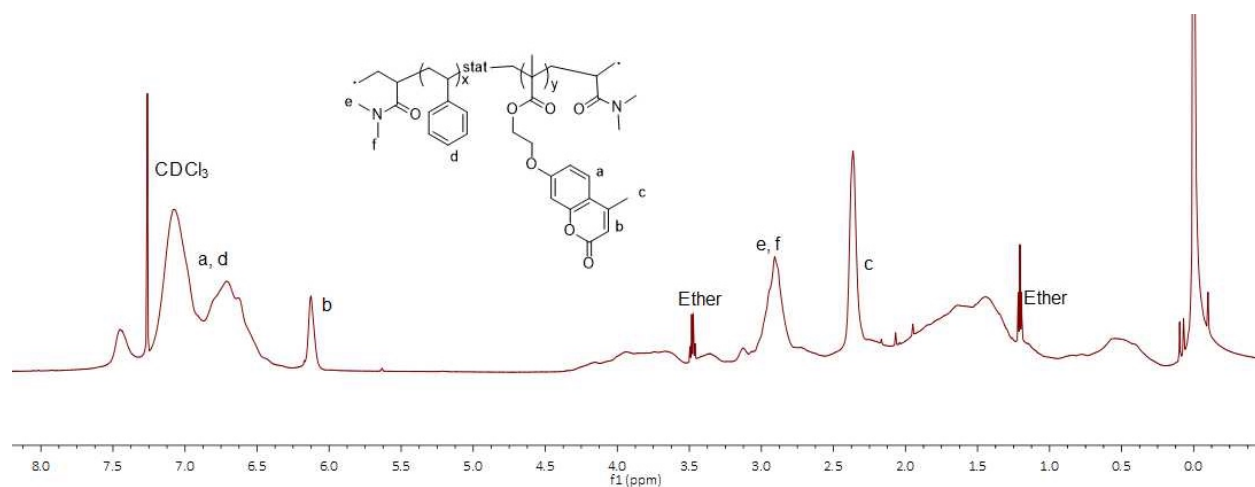
NMR Analysis of PDMA-PS-*stat*-PCMA-PDMA

Figure A6. NMR of PDMA-PS-*stat*-PCMA-PDMA

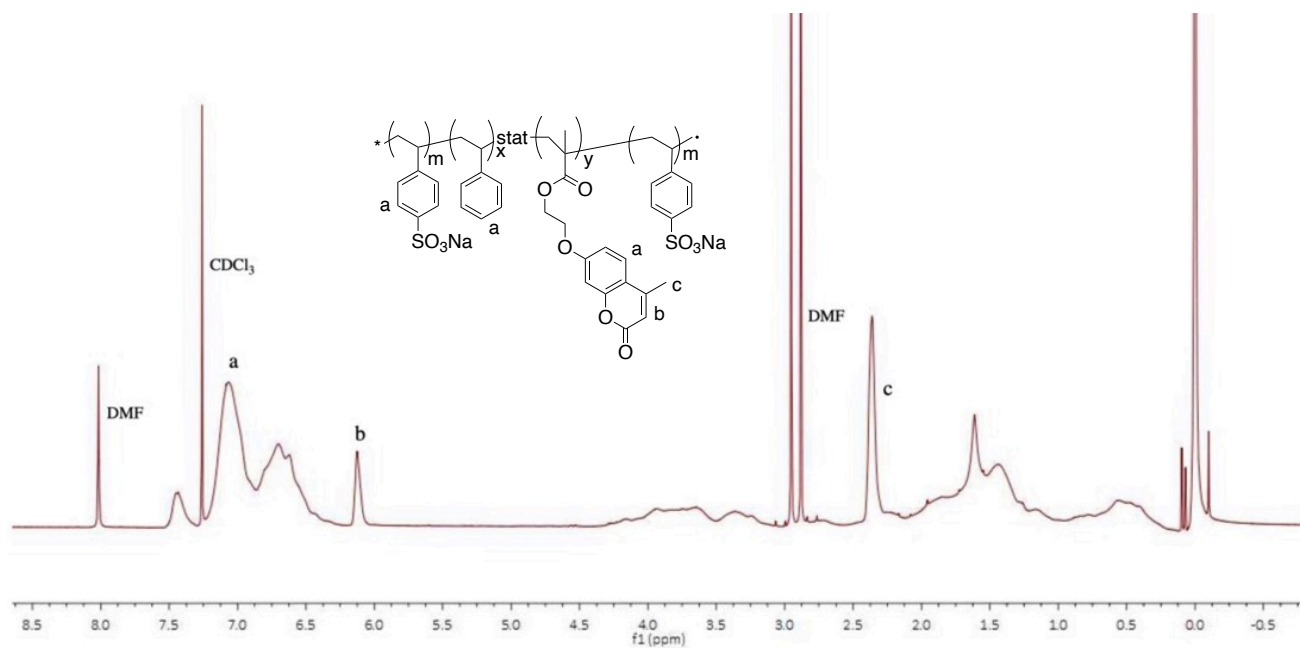NMR Analysis of NaSS-PS-*stat*-pCMA-NaSS

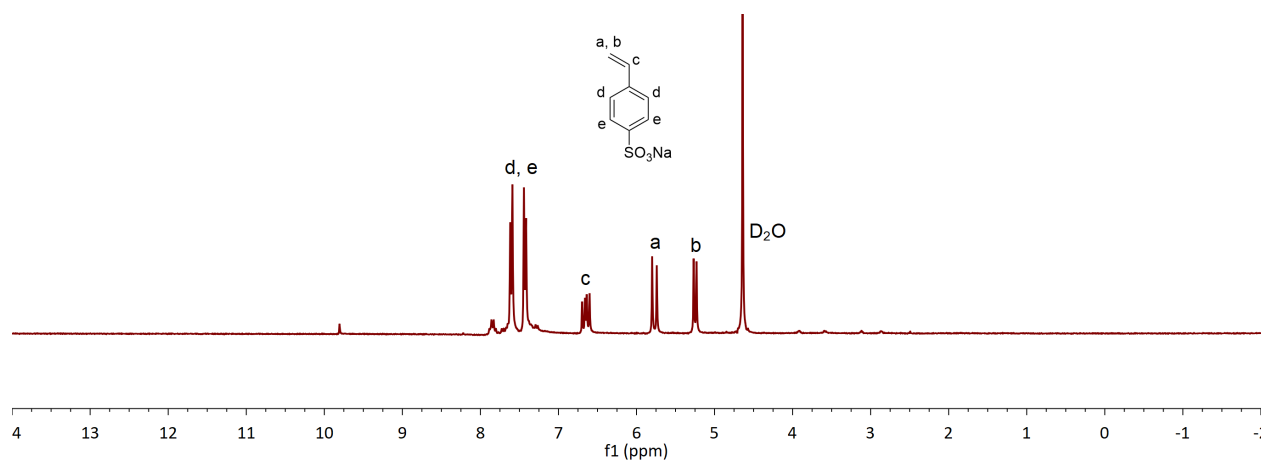**Figure A7**. NMR of PNaSS-PS-*stat*-PCMA-PNaSS
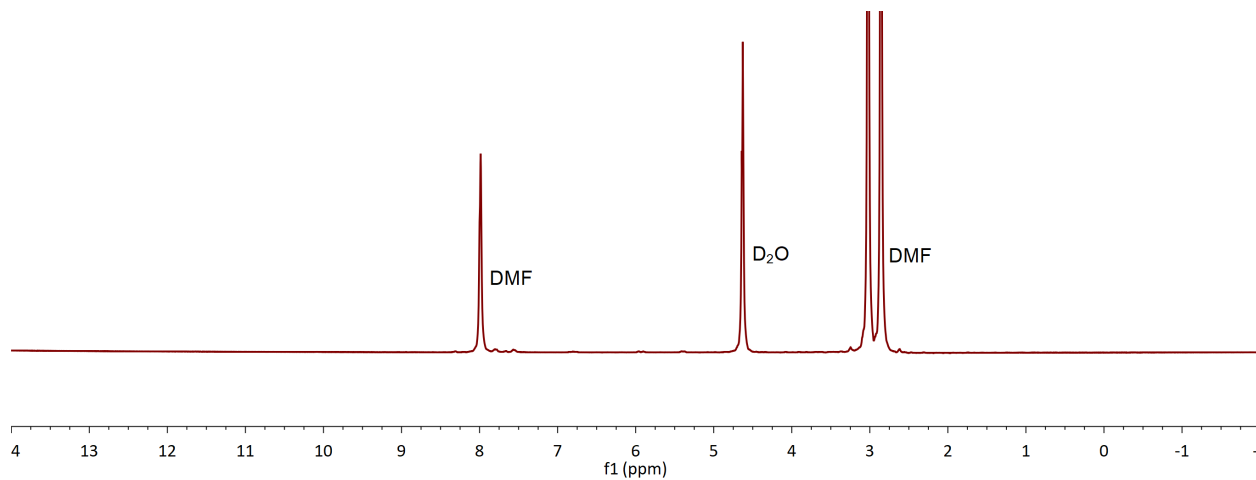

Figure A8. NMR of NaSS monomer

Figure A9. NMR of the solution in which PNaSS-PS-*stat*-PCMA-PNaSS had precipitated